AD-A065 589 OHIO STATE UNIV COLUMBUS ELECTROSCIENCE LAB F/G 9/5
WING-MOUNTED ANTENNA CODE - USER'S MANUAL.(U)
MAY 78 R J MARHEFKA, W D BURNSIDE N62269-76-C-0554
UNCLASSIFIED ESL-(78)4583-5 NADC-79044-30 NL

1 OF 1
AD
AO 65589

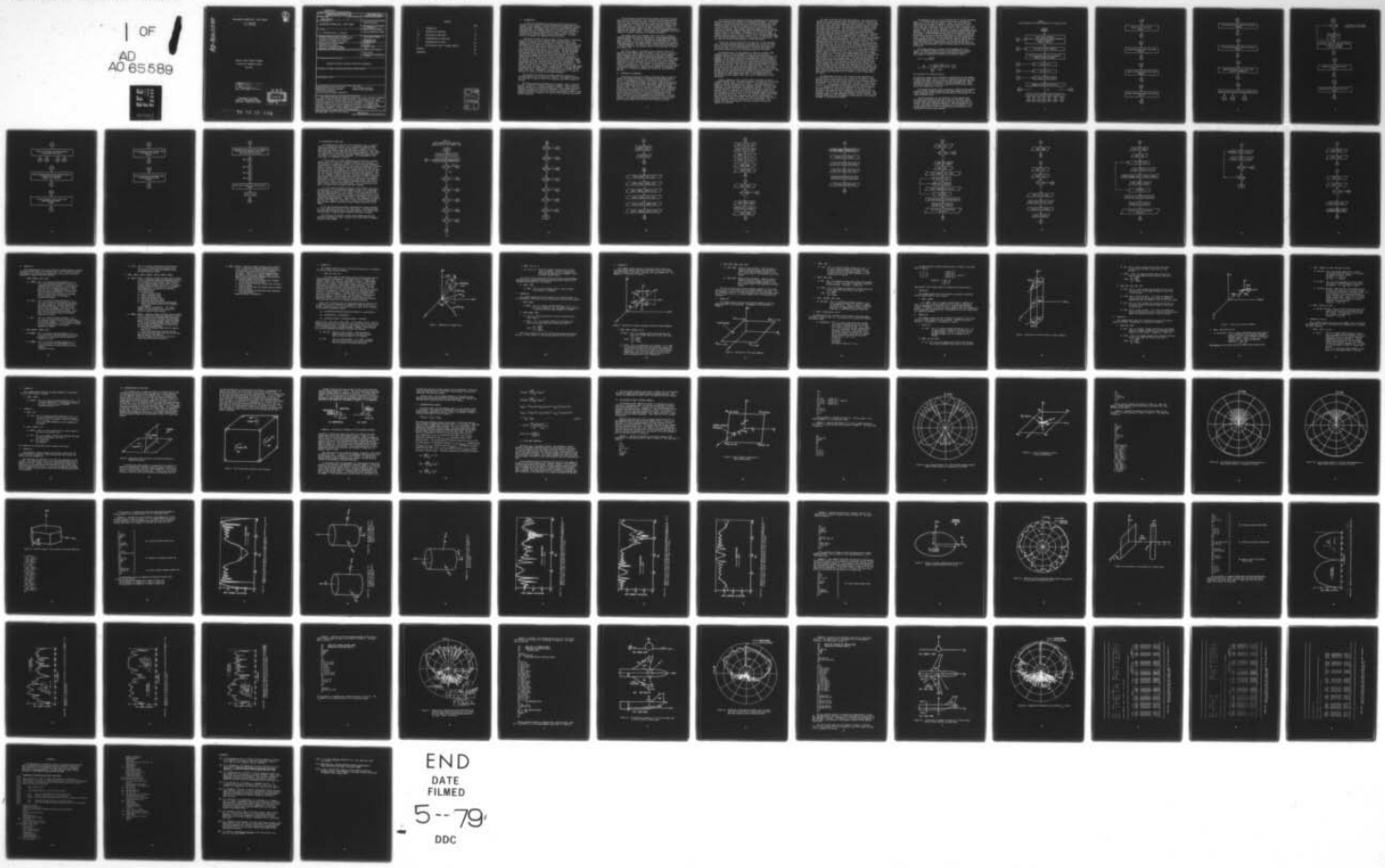

END
DATE FILMED
5-79
DDC

AD-A065589

1 LEVEL II

WING-MOUNTED ANTENNA CODE - USER'S MANUAL

R. J. Marhefka
W. D. Burnside

Technical Report 4583-5 (784583)

Contract No. N62269-76-C-0554

May 1978

DISTRIBUTION STATEMENT A
Approved for public release;
Distribution Unlimited

Department of the Navy
Naval Air Development Center
Warminster, Pennsylvania 18974

DDC
RECEIVED
13 MAR 1979
E

79 03 12 149

UNCLASSIFIED

SECURITY CLASSIFICATION OF THIS PAGE *(When Data Entered)*

REPORT DOCUMENTATION PAGE		READ INSTRUCTIONS BEFORE COMPLETING FORM
1. REPORT NUMBER NADC-79044-30	2. GOVT ACCESSION NO.	3. RECIPIENT'S CATALOG NUMBER
4. TITLE *(and Subtitle)* WING-MOUNTED ANTENNA CODE - USER'S MANUAL		5. TYPE OF REPORT & PERIOD COVERED Technical Report
		6. PERFORMING ORG. REPORT NUMBER ESL (78)4583-5
7. AUTHOR(s) R. J. Marhefka and W. D. Burnside		8. CONTRACT OR GRANT NUMBER(s) Contract N62269-76-C-0554
9. PERFORMING ORGANIZATION NAME AND ADDRESS The Ohio State University ElectroScience Laboratory, Department of Electrical Engineering, Columbus, Ohio 43212		10. PROGRAM ELEMENT, PROJECT, TASK AREA & WORK UNIT NUMBERS 63206N, WR6-1154 WTW180000, RA702
11. CONTROLLING OFFICE NAME AND ADDRESS Department of the Navy Naval Air Development Center Warminster, Pennsylvania 18974		12. REPORT DATE May 1978 13. NUMBER OF PAGES 83
14. MONITORING AGENCY NAME & ADDRESS*(if different from Controlling Office)*		15. SECURITY CLASS. *(of this report)* Unclassified 15a. DECLASSIFICATION/DOWNGRADING SCHEDULE

16. DISTRIBUTION STATEMENT *(of this Report)*

Approved for public release; distribution unlimited

17. DISTRIBUTION STATEMENT *(of the abstract entered in Block 20, if different from Report)*

18. SUPPLEMENTARY NOTES

19. KEY WORDS *(Continue on reverse side if necessary and identify by block number)*

Antennas near aircraft structures
Approximate aircraft structures
Flat plate simulations
Finite elliptic cylinder simulations
High frequency solution
Computer code description

20. ABSTRACT *(Continue on reverse side if necessary and identify by block number)*

This report provides the necessary information to run a Fortran IV computer code which is used to analyze antenna patterns. The antenna can be in the presence of various structures which can be simulated by finite flat plates, an infinite ground plane, and a finite elliptic cylinder. For example, the radiation pattern of an antenna mounted on the wing of an aircraft can be analyzed. The computer code is theoretically based on the Geometrical Theory of Diffraction approach. Various examples are presented to illustrate the versatility of the code as well as its subtleties.

DD FORM 1 JAN 73 1473 EDITION OF 1 NOV 65 IS OBSOLETE

UNCLASSIFIED

SECURITY CLASSIFICATION OF THIS PAGE *(When Data Entered)*

CONTENTS

ACCESSION for
NTIS White Section
DDC Buff Section
UNANNOUNCED
JUSTIFICATION
BY
DISTRIBUTION/AVAILABILITY CODES
Dist. AVAIL. and/or SPECIAL
A

I. INTRODUCTION

In order to investigate the scattering effects associated with antennas in the presence of complex scattering structures such as wing-mounted aircraft antennas, the following Fortran IV computer code has been developed. The computer code is used to compute the far-zone scattered fields for antennas radiating in the near zone of perfectly-conducting structures simulated by flat plates, a finite elliptic cylinder and an infinite ground plane at and above UHF. The code is based on the geometrical theory of diffraction (GTD).

The code will allow the user to model a large variety of scattering structures using the basic structural model mentioned above. For example, an aircraft can be simulated by a finite elliptic cylinder fuselage with flat plate wings, engines, and stores. Alternatively, the flat plates can be used alone to represent rectangular boxes, pyramids, etc. for ground stations and the finite elliptic cylinder can be used to represent masts, smoke stacks, etc. on ships. The infinite ground plane can be used to simulate multipath effects. The code calculates the scattered fields from the individual structures and the major coupling terms between the plates and elliptic cylinder (i.e., by including double interactions such as double reflection, reflection-diffraction, etc.). Note that the plate and cylinder structures shadow one another, such that discontinuities can appear in the pattern. These discontinuities result from neglecting higher order interactions. These higher-order terms are normally negligible and can only effect the pattern in small sectors. However, if they are significant in some region, a discontinuity will appear in the computed pattern. The amplitude jump associated with the discontinuity is indicative of the strength of the higher-order term. Consequently, when the solution fails, it tends to indicate its failure in terms of the observed pattern.

The code has the flexibility to handle arbitrary pattern cuts. Volumetric patterns can be obtained if desired. This numerical solution can, therefore be used to solve a very large and significant number of problems.

The antenna presently considered in the computer code is simulated by a set of electric or magnetic elemental radiators. Each electric or magnetic radiator has a cosine distribution, arbitrary length, arbitrary magnitude and phase, and arbitrary orientation. Any antenna type can therefore be analyzed as long as the current distribution is known. Other elemental antennas or methods can be used by simply modifying the antenna pattern subroutine.

The limitations associated with the computer code result from the basic nature of the analyses. The solution is derived using the GTD, which is a high frequency approach. In terms of the scattering from plate structures this means that each plate should have edges at least a wavelength long. In terms of the cylinder structure its major and minor radii and length sould be at least a wavelength in extent. In addition, each antenna element should be at least a wavelength from all edges and the curved surface. In many cases, the wavelength limit can be reduced to a quarter wavelength for engineering purposes.

The present form of the computer code is not large in terms of computer storage and executes a pattern for a single antenna element very efficiently. The present code requires approximately 200 to 300 K bytes of storage. It will run a pattern cut of 360 points for a flat plate structure with one antenna element in approximately 10 seconds on a CDC-6600 computer. The code will run a pattern cut of 360 points for a finite cylinder with one antenna element in approximately 30 seconds on a Univac 1110.

This user's manual is designed to give an overall view of the operation of the computer code, to instruct a user in how to use it to model structures, and to show the validity of the code by comparing various computed results against measured data whenever available. Section II describes an overall view of the organization of the program. The definition of the input is given in Section III. How to apply the capabilities of this input data to a practical structure is briefly discussed in Section IV. This includes a clarification of the subtle points of interpreting the input data. The representation of the output is discussed in Section V. Various sample problems are presented in Section VI to illustrate the operation, versatility, and validity of the code.

II. PRINCIPLES OF OPERATION

The analytical modeling of complex scattering shapes in order to predict the radiation patterns of antennas has been accomplished by the use of the Geometrical Theory of Diffraction (GTD) [1,2,3]. This is a high frequency technique that allows a complicated structure to be approximated by basic shapes representing canonical problems in the GTD. These shapes include flat and curved wedges and convex curved surfaces. The GTD is a ray optical technique and it therefore allows one to gain some physical insight into the various scattering and diffraction mechanisms involved. Consequently, one is able to quickly seek out the dominant or significant scattering and diffraction mechanism for a given geometrical configuration. This, in turn, leads to an accurate engineering solution to practical antenna problems. This approach has been used successfully in the past to model aircraft shapes [4,5] and ship-like structures [6,7,8].

This section briefly describes the basic operation of this scattering code for the analysis of antennas in an aircraft environment. The present version of the code allows analysis of scattering structures that can be modeled by concave flat plate structures, an infinite ground plane, and a finite elliptic cylinder all of which are built up from the basic canonical structures. These shapes allow one to model a wide variety of structures in the UHF range and above where the scattering structures are large in terms of a wavelength. The general rule is that the lower frequency limit of this solution is dictated by the spacings between the various scattering centers and their overall size. In practice this means that the smallest dimensions should be on the order of a wavelength. This can often be relaxed to approximately a quarter-wavelength.

The positive time convention $e^{j\omega t}$ has been used in this scattering code. Also, the radiation patterns are assumed to be in the far field. The term e^{-jkR}/R has been suppressed unless otherwise specified by the user of the code. All of the structures in this code are assumed to be perfectly conducting and the surrounding medium is free space.

As mentioned above, the GTD approach is ideal for a general high frequency study of aircraft antennas in that only the most basic structural features of an otherwise very complicated structure need to be modeled. This is because ray optical techniques are used to determine components of the field incident on and diffracted by various structures. Components of the diffracted fields are found using the GTD solutions in terms of the individual rays which are summed with the geometrical optics terms in the far field. The rays from a given scatterer tend to interact with other structures causing various higher-order terms. In this way one can trace out the various possible combinations of rays that interact between scatterers and determine and include only the dominant terms. Thus, one need only be concerned with the important scattering components and neglect all other higher-order terms. This method leads to accurate and efficient computer codes that can be systematically written and tested.

Complex problems are built up from similar components in terms of a modular computer code. This modular approach is illustrated in the block diagram of the main program shown in Table I. The scattering code is broken up into many subroutines that represent different scattered field components, ray tracing methods, and shadowing routines. As can be seen from the flow chart, the code is structured so that all of one type of scattered field is computed at one time for the complete pattern cut so that the amount of core swapping is minimized thereby reducing overlaying and increasing efficiency. This also is an important feature that allows the code to be used on small computers that are not large enough to accept the entire code at one time. The code can be broken into smaller overlay segments which will individually fit in the machine. The results are, then, superimposed in the main program as the various segments are executed.

The code is divided into three large sections. The first section contains the major scattered fields associated with the individual flat plates and the interactions between the different plates. These include the direct field, the singly reflected fields, doubly reflected fields, the singly diffracted fields, the reflected-diffracted fields, and the diffracted-reflected fields. The diffracted fields include the normal diffracted fields as well as slope diffraction, a newly developed heuristic corner diffracted field and slope-corner diffracted field. The double diffracted fields are not included at present, but a warning is provided wherever this field component might be important. This is usually only a small angular section of space. This field may be included later whenever time and effort permit. The second section contains the major scattered fields associated with the elliptic cylinder. This includes the direct field, if not already computed in the plate section, the reflected field, the transition field, the deep shadow fields, the reflected field from the end caps, and the diffracted field from the end cap rims. The diffracted field from the end cap rim is not at present corrected in the pseudo caustic regions. This is where three diffraction points on the rim coalesce into one. This is only important in small angular regions in space and is not deemed appropriate to be included at the present time. An equivalent current method could be used for this small region but it is rather time consuming to use for the benefits derived from it for such a general code. The third section contains the major scattered fields associated with the interactions between the plates and cylinder. This includes, at present, the fields reflected from the plates then reflected or diffracted from the cylinder, the fields reflected from the cylinder then reflected from the plates, the fields reflected from the cylinder then diffracted from the plates, and the fields diffracted from the plates then reflected from the cylinder. These terms have been found to be sufficient for engineering purposes when analyzing wing-mounted aircraft antennas as well as many other structures.

The subroutines for each of the scattered field components are all structured in the same basic way. First, the ray path is traced backward from the chosen observation direction to a particular scatterer and subsequently to the source using either the laws of reflection or diffraction. Each ray path, assuming one is possible, is then checked to see if it is shadowed by any structure along the complete ray path. If it is shadowed the field is not computed and the code proceeds to the next scatterer or observation direction. If the path is not interrupted the scattered field is computed using the appropriate GTD solutions. The fields are then superimposed in the main program. This shadowing process is often speeded up by making various decisions based on bounds associated with the geometry of the structure. This type of knowledge is used wherever possible.

The shadowing of rays is a very important part of the GTD scattering code. It is obvious that this approach should lead to various discontinuities in the resulting pattern. However, the GTD diffraction coefficients are designed to smooth out the discontinuities in the fields such that a continuous field is obtained. When a scattered field is not included in the result, therefore, the lack of its presence is apparent. This can be used to advantage in analyzing complicated problems. Obviously in a complex problem not all the possible scattered fields can be included. In the GTD code the importance of the neglected terms are determined by the size of the so-called gliches or jumps in the pattern trace. If the gliches are small no additional terms are needed for a good engineering solution. If the gliches are large it may be necessary to include more terms in the solution. In any case the user has a gauge with which he can examine the accuracy of the results and is not falsely led into believing a result is correct when in fact there could be an error.

The antenna presently considered in the computer code is an electric or magnetic radiator with a cosine distribution, arbitrary length, arbitrary magnitude and phase, and arbitrary orientation. This antenna is specified as follows for an electric dipole:

$$I(z') = I_m \cos\left(\frac{\pi z'}{\ell}\right)$$

$$E_{\theta'} = \frac{jn_o}{2\pi} I_m \frac{\sin\theta' \left(\frac{\pi}{k\ell}\right) \cos\left(\frac{k\ell}{2} \cos\theta'\right)}{\left(\frac{\pi}{k\ell}\right)^2 - \cos^2\theta'} \frac{e^{-jkr'}}{r'}$$

and similarly for a magnetic dipole.

Any arbitrary antenna can be simulated by superposition of the elements by making the length ℓ small ($\ell \lesssim 0.1\lambda$), spacing the elements less than a quarter wavelength, and then weighting their magnitudes and phases to simulate the current distribution of the desired antenna [9]. Since the radiation pattern is relatively insensitive to the current distribution this method works very well.

Even though the present code is based on a standard dipole antenna, it can be easily changed by modifying the SOURCE subroutine and the SOURCP subroutine, which contains the derivative of the pattern for the slope diffracted fields.

The brief discussion of the operation of the scattering code given above should help the user get a feel for the overall code so he might better understand the code's capabilities and interpret its results. The code is designed, however, so that the general user can run the code without knowing all the details of its operation. Yet, he must become familiar with the input/output details which will be discussed in the next three sections.

TABLE I
Block Diagram of the Main Program for the Computer Code

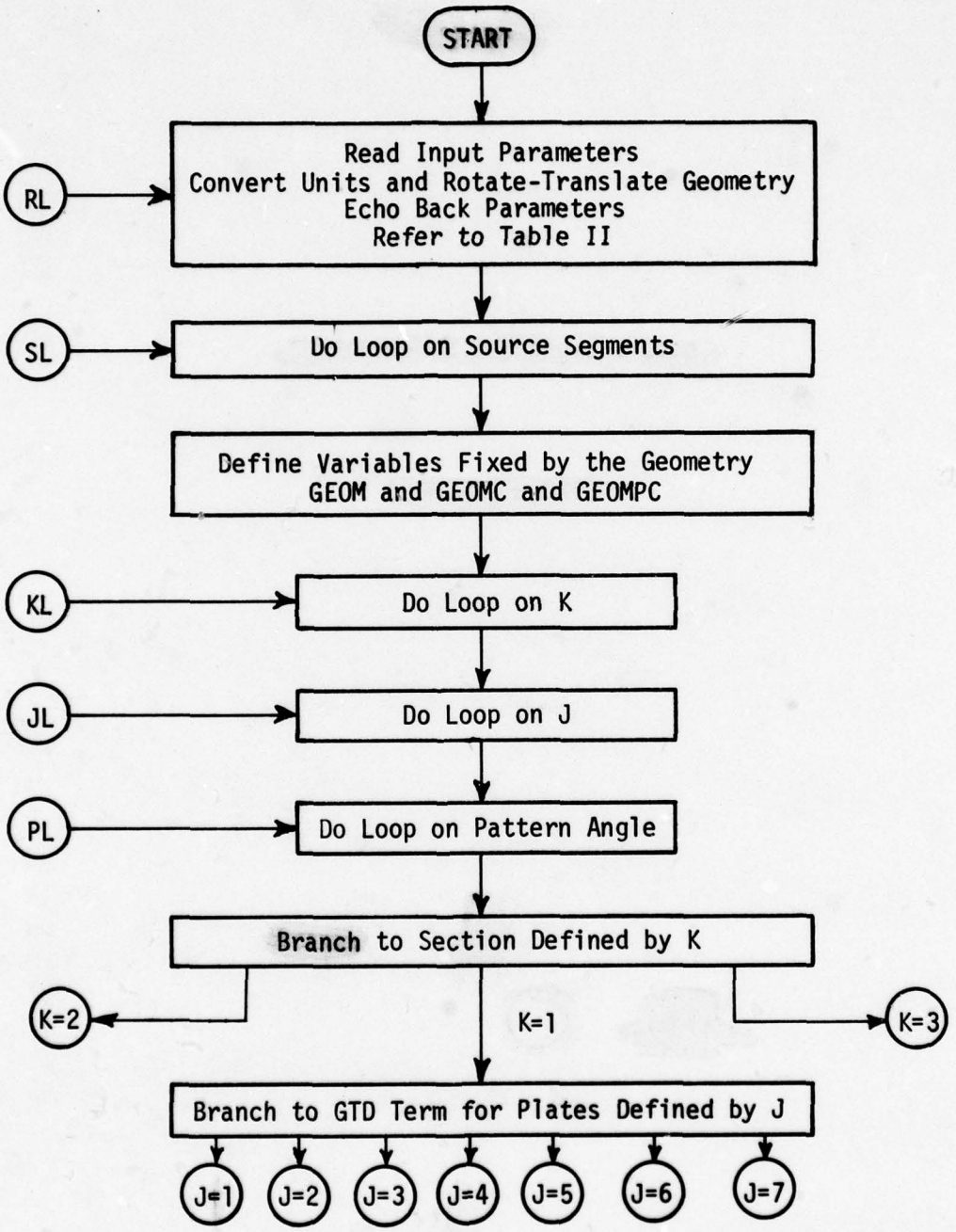

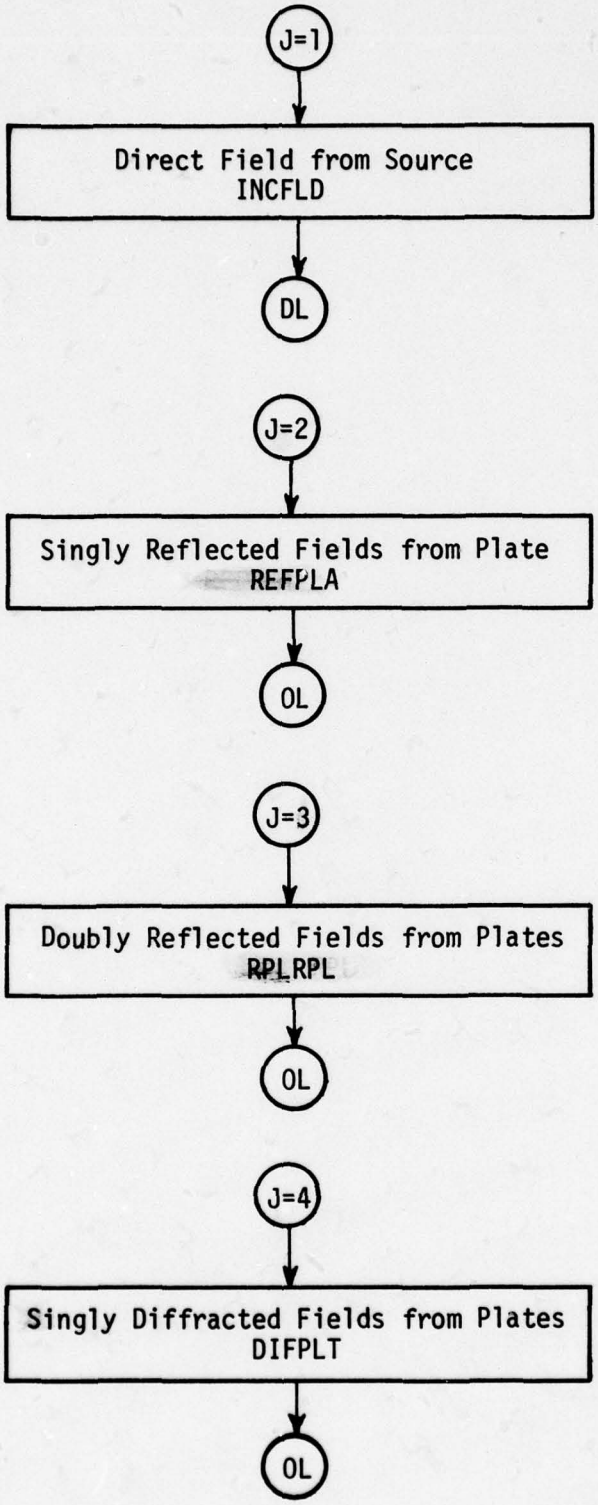
J=1
Direct Field from Source
INCFLD
DL
J=2
Singly Reflected Fields from Plate
REFPLA
OL
J=3
Doubly Reflected Fields from Plates
RPLRPL
OL
J=4
Singly Diffracted Fields from Plates
DIFPLT
OL

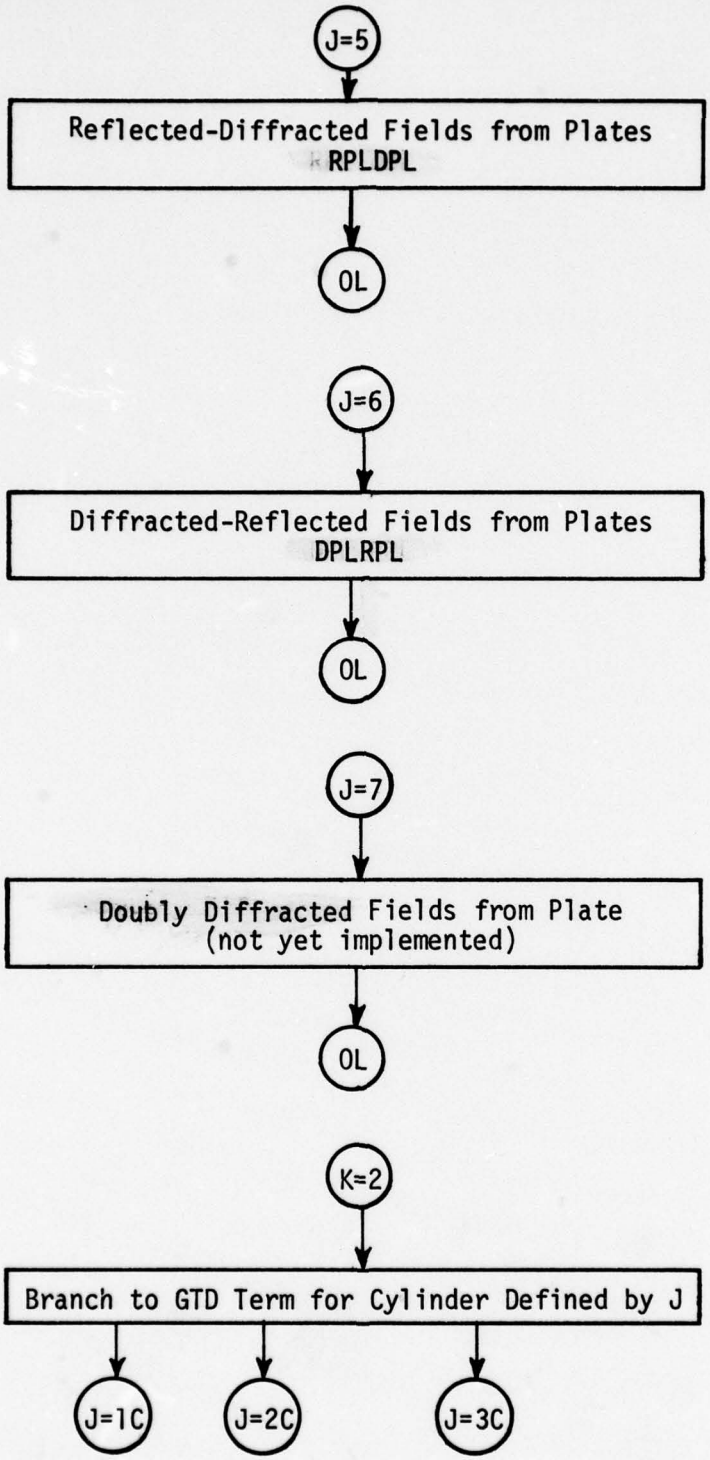
J=5
Reflected-Diffracted Fields from Plates
RPLDPL
OL
J=6
Diffracted-Reflected Fields from Plates
DPLRPL
OL
J=7
Doubly Diffracted Fields from Plate
(not yet implemented)
OL
K=2
Branch to GTD Term for Cylinder Defined by J
J=1C
J=2C
J=3C

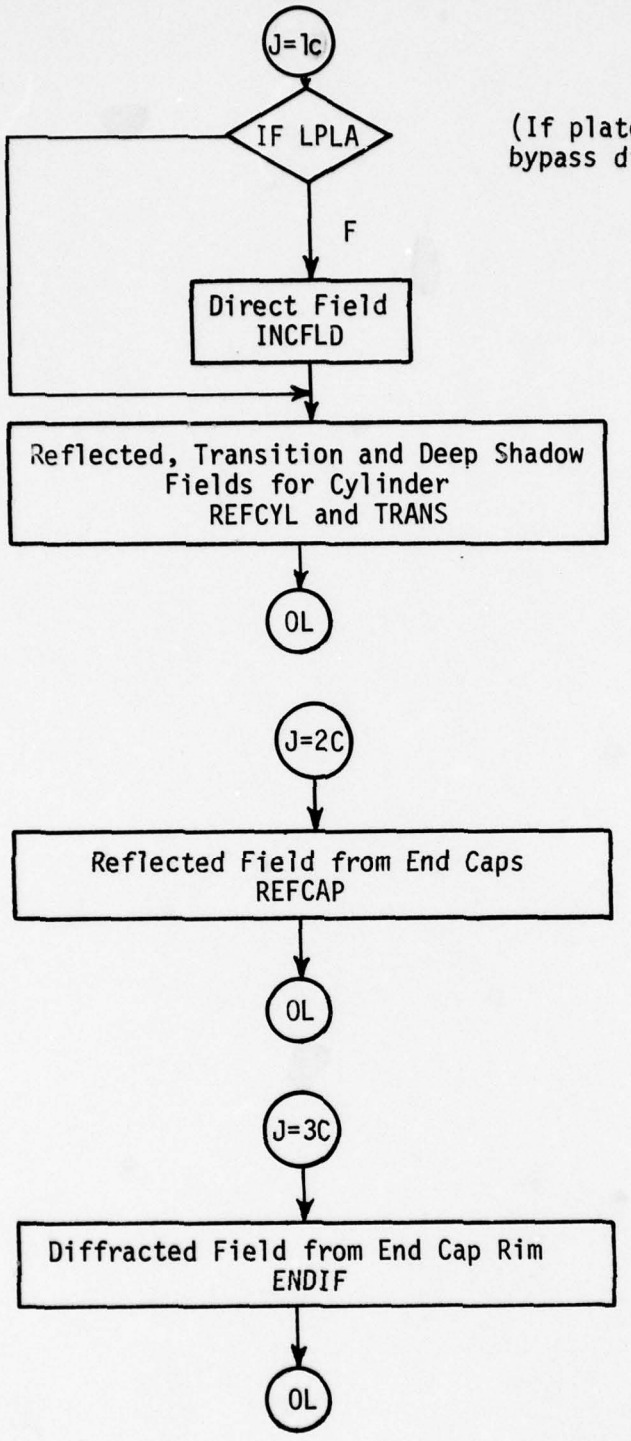

(If plate is also present bypass direct field here)

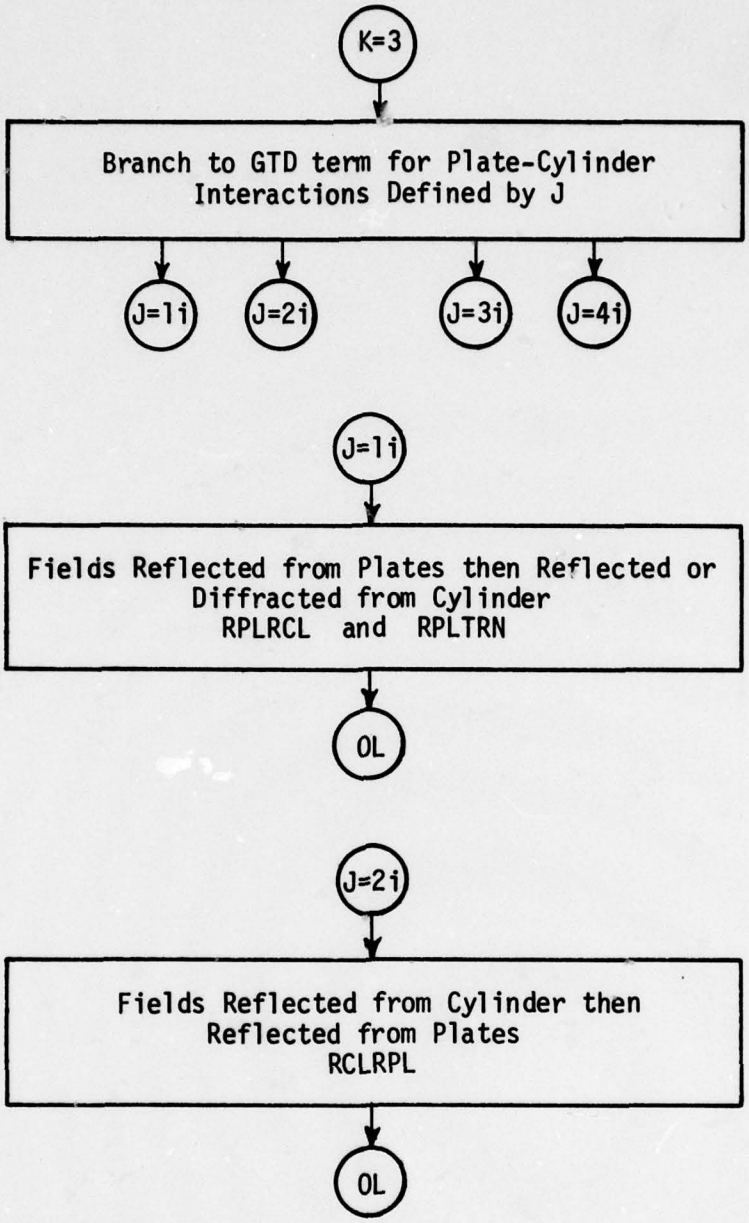
K=3
Branch to GTD term for Plate-Cylinder Interactions Defined by J
J=1i
J=2i
J=3i
J=4i
J=1i
Fields Reflected from Plates then Reflected or Diffracted from Cylinder
RPLRCL and RPLTRN
OL
J=2i
Fields Reflected from Cylinder then Reflected from Plates
RCLRPL
OL

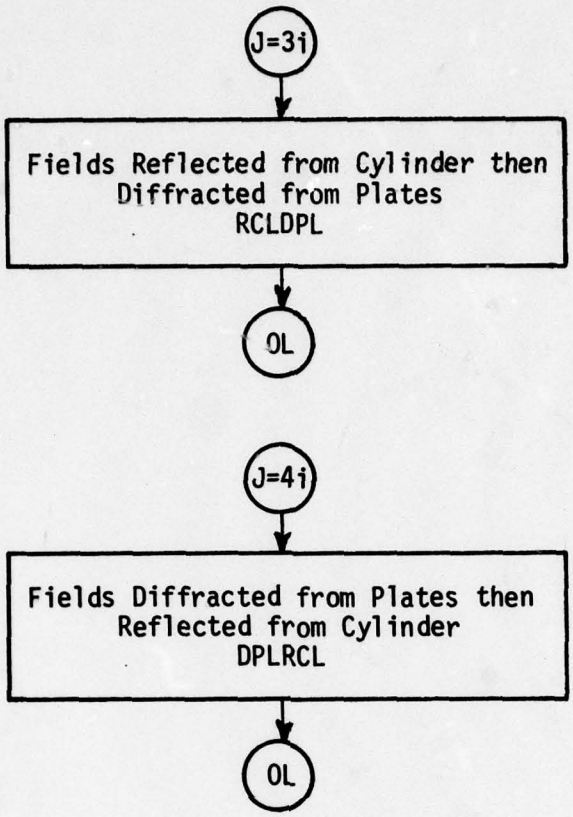
J=3i
Fields Reflected from Cylinder then Diffracted from Plates
RCLDPL
OL
J=4i
Fields Diffracted from Plates then Reflected from Cylinder
DPLRCL
OL

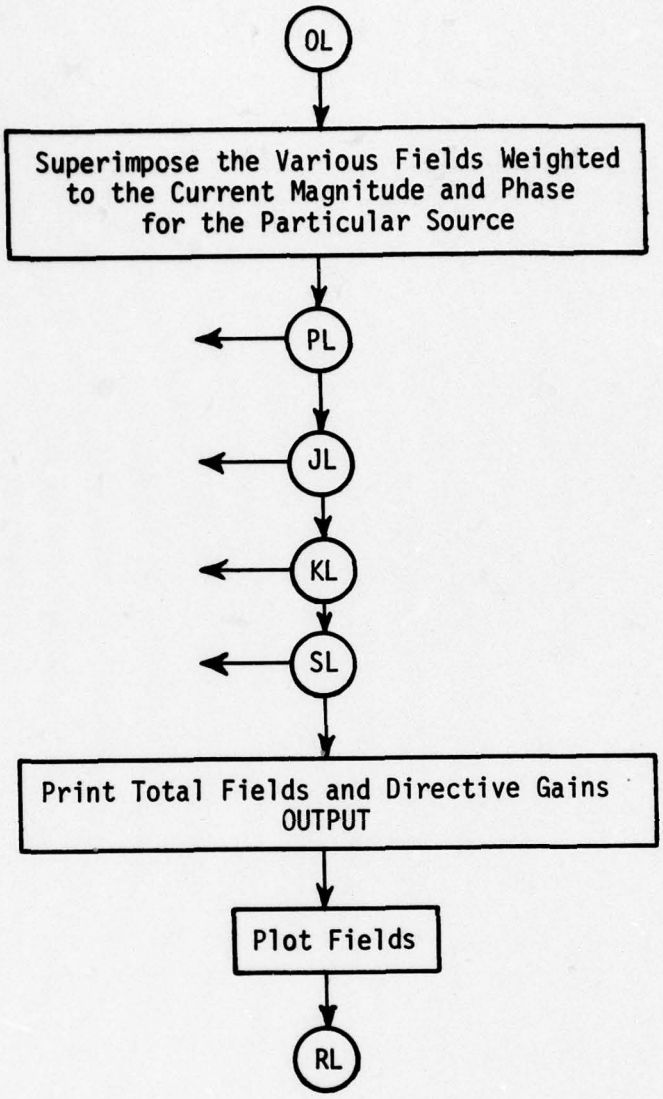
OL
Superimpose the Various Fields Weighted to the Current Magnitude and Phase for the Particular Source
PL
JL
KL
SL
Print Total Fields and Directive Gains OUTPUT
Plot Fields
RL

III. DEFINITION OF INPUT DATA

The method used to input data into the computer code is presently based on a command word system. This is especially convenient when more than one problem is to be analyzed during a computer run. The code stores the previous input data such that one need only input that data which needs to be changed from the previous execution. Also, there is a default list of data so for any given problem the amount of data that needs to be input has been shortened. The organization of the input data is illustrated in Table II.

In this system, all linear dimensions may be specified in either meters, inches, or feet and all angular dimensions are in degrees. All the dimensions are eventually referred to a fixed cartesian coordinate system used as a common reference for the source and scattering structures. There is, however, a geometry definition coordinate system that may be defined using the "RT:" command. This command enables the user to rotate and translate the coordinate system to be used to input any select data set into the best coordinate system for that particular geometry. Once the "RT:" command is used all the input following the command will be in that rotated and translated coordinate system until the "RT:" command is called again. The only exception to this is that the infinite ground plane will always be in the reference coordinate system. See below for more details. There is also a separate coordinate system that can be used to define a pattern coordinate system. This is discussed in more detail in section III-B in terms of the "PD:" command.

It is felt that the maximum usefulness of the computer code can be achieved using it on an interactive computer system. As a consequence, all input data are defined in free format such that the operator need only put commas between the various inputs. This allows the user on an interactive terminal to avoid the problems associated with typing in the field length associated with a fixed format. This method also is useful on batch processing computers. Note that all read statements are made on unit #5, i.e., READ (5,-), where the "-" symbol refers to free format. Other machines, however, may have different symbols representing free format.

In all the following discussions associated with logical variables a "T" will imply true, and an "F" will imply false. The complete words true and false need not be input since most compilers just consider the first character in determining the state of the logical variable.

The following list defines in detail each command word and the variables associated with them. Section VI will give specific examples using this input method.

TABLE II
Block Diagram of the Input Data
Organization for the Computer Code

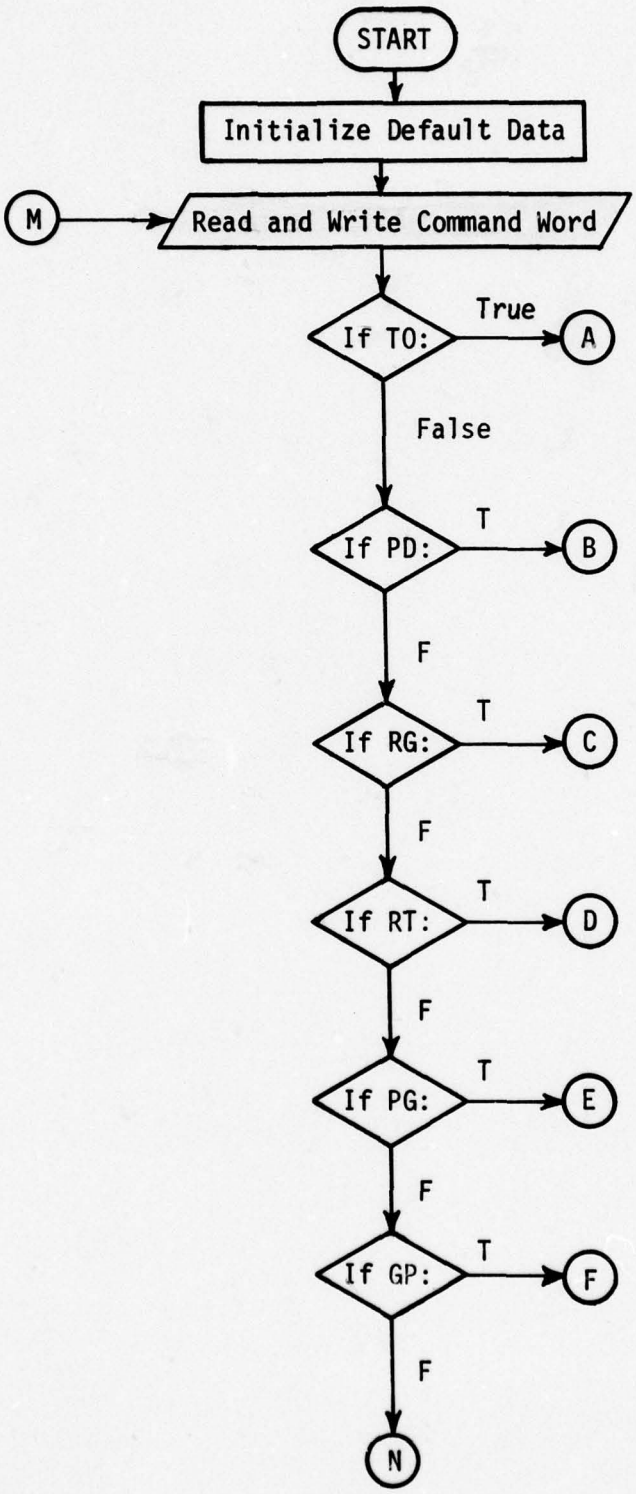

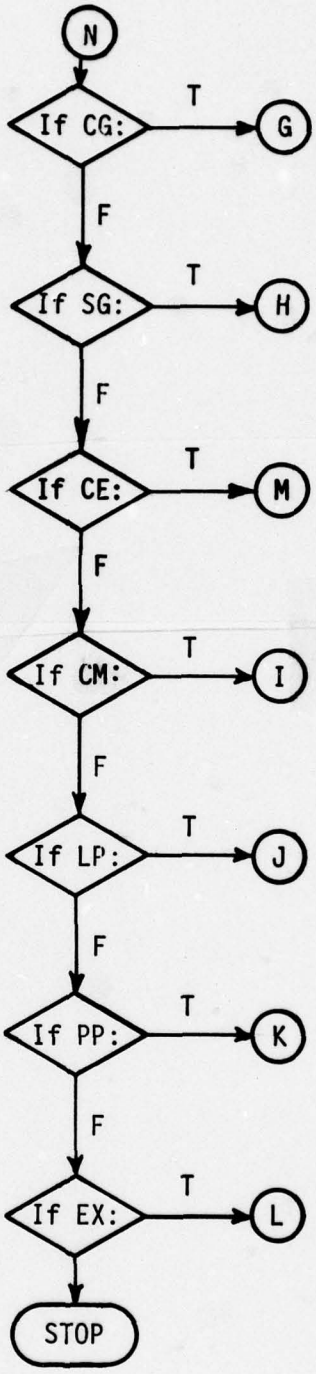
N
If CG:
T
G
F
If SG:
T
H
F
If CE:
T
M
F
If CM:
T
I
F
If LP:
T
J
F
If PP:
T
K
F
If EX:
T
L
STOP

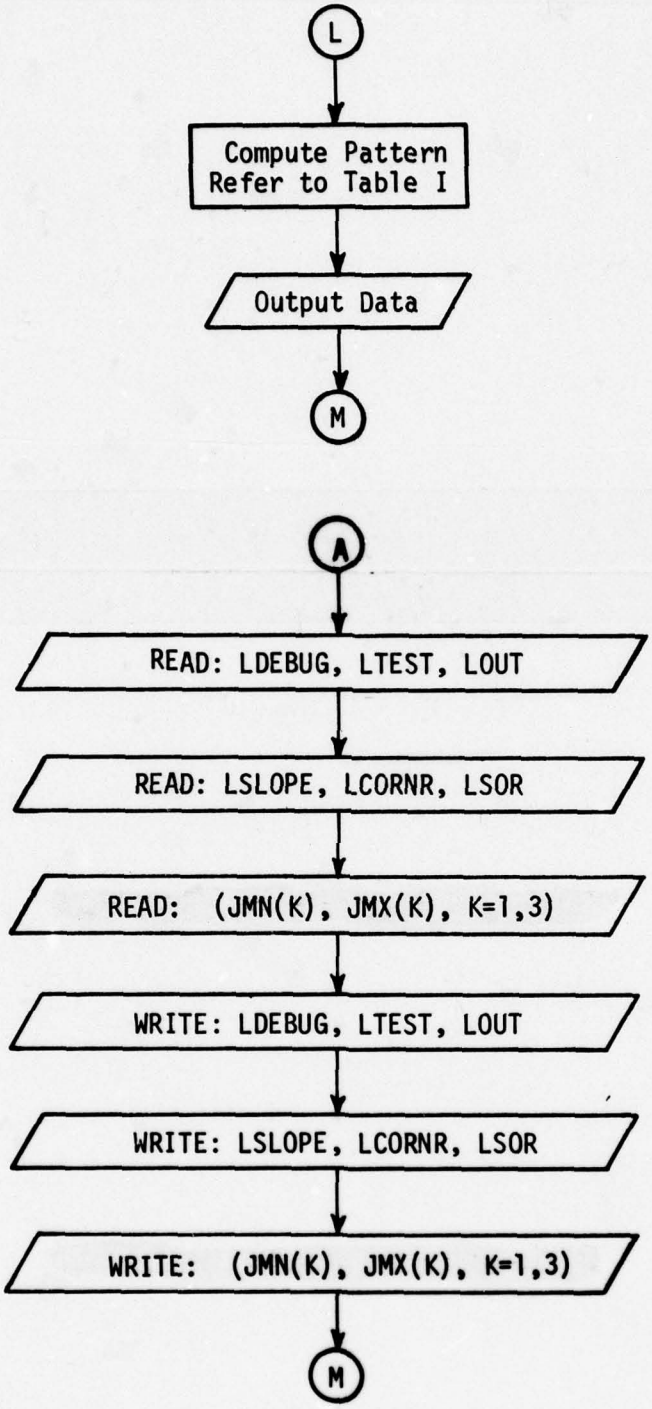
L
Compute Pattern
Refer to Table I
Output Data
M
A
READ: LDEBUG, LTEST, LOUT
READ: LSLOPE, LCORNR, LSOR
READ: (JMN(K), JMX(K), K=1,3)
WRITE: LDEBUG, LTEST, LOUT
WRITE: LSLOPE, LCORNR, LSOR
WRITE: (JMN(K), JMX(K), K=1,3)
M

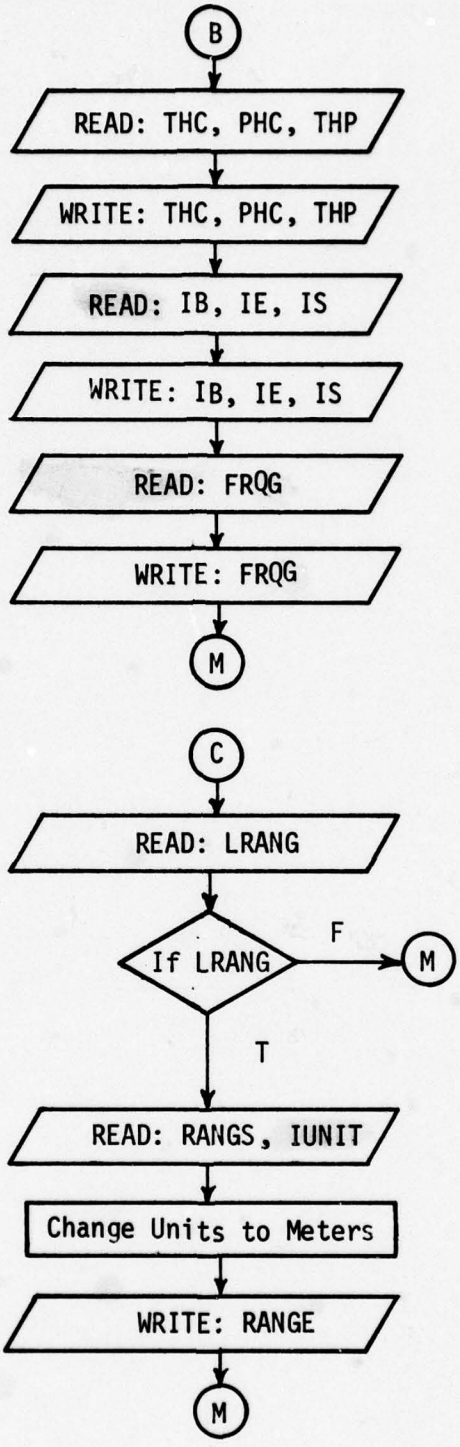
B
READ: THC, PHC, THP
WRITE: THC, PHC, THP
READ: IB, IE, IS
WRITE: IB, IE, IS
READ: FRQG
WRITE: FRQG
M
C
READ: LRANG
If LRANG
F
M
T
READ: RANGS, IUNIT
Change Units to Meters
WRITE: RANGE
M

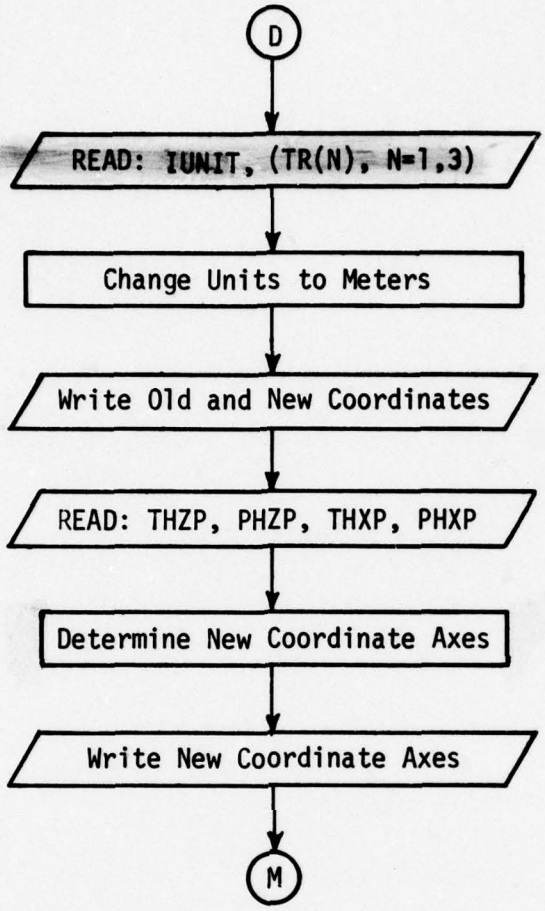
D
READ: IUNIT, (TR(N), N=1,3)
Change Units to Meters
Write Old and New Coordinates
READ: THZP, PHZP, THXP, PHXP
Determine New Coordinate Axes
Write New Coordinate Axes
M

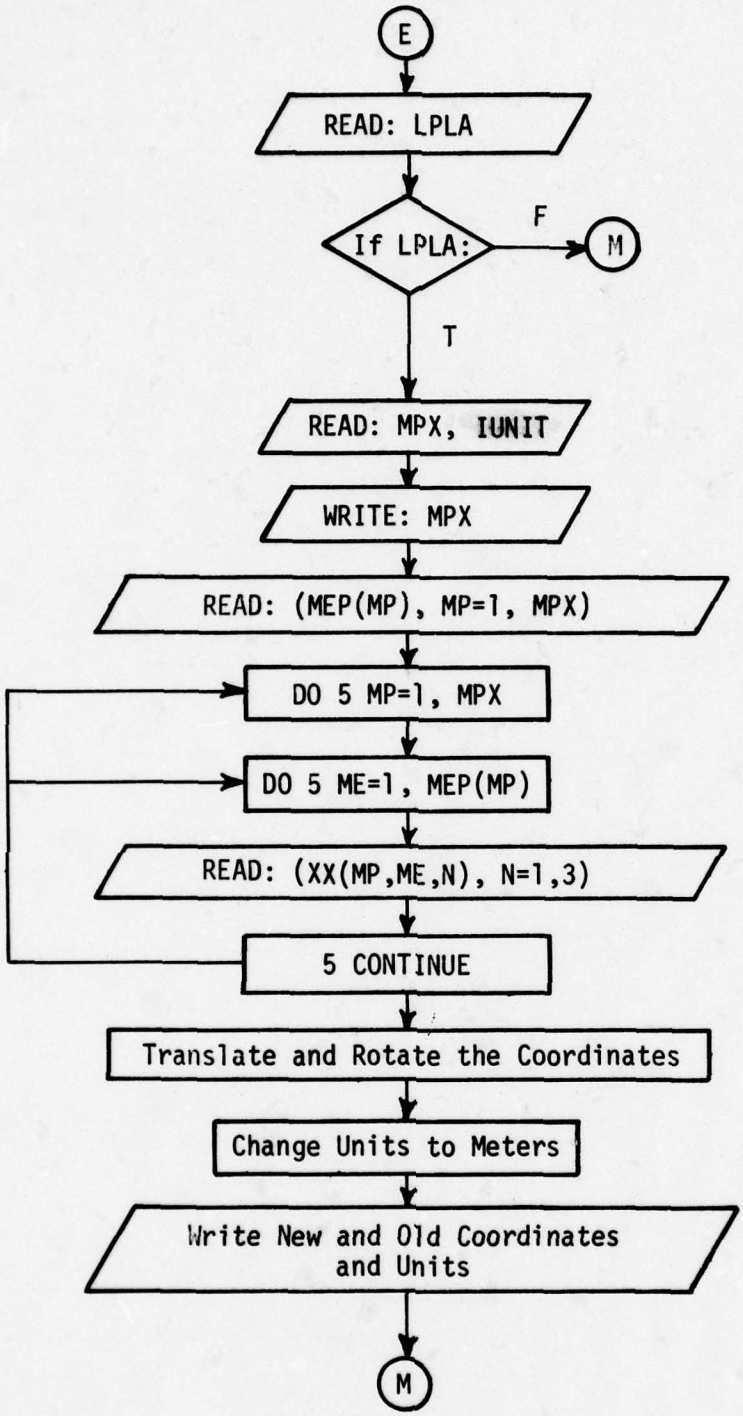
E
READ: LPLA
If LPLA:
F
M
T
READ: MPX, IUNIT
WRITE: MPX
READ: (MEP(MP), MP=1, MPX)
DO 5 MP=1, MPX
DO 5 ME=1, MEP(MP)
READ: (XX(MP,ME,N), N=1,3)
5 CONTINUE
Translate and Rotate the Coordinates
Change Units to Meters
Write New and Old Coordinates
and Units
M

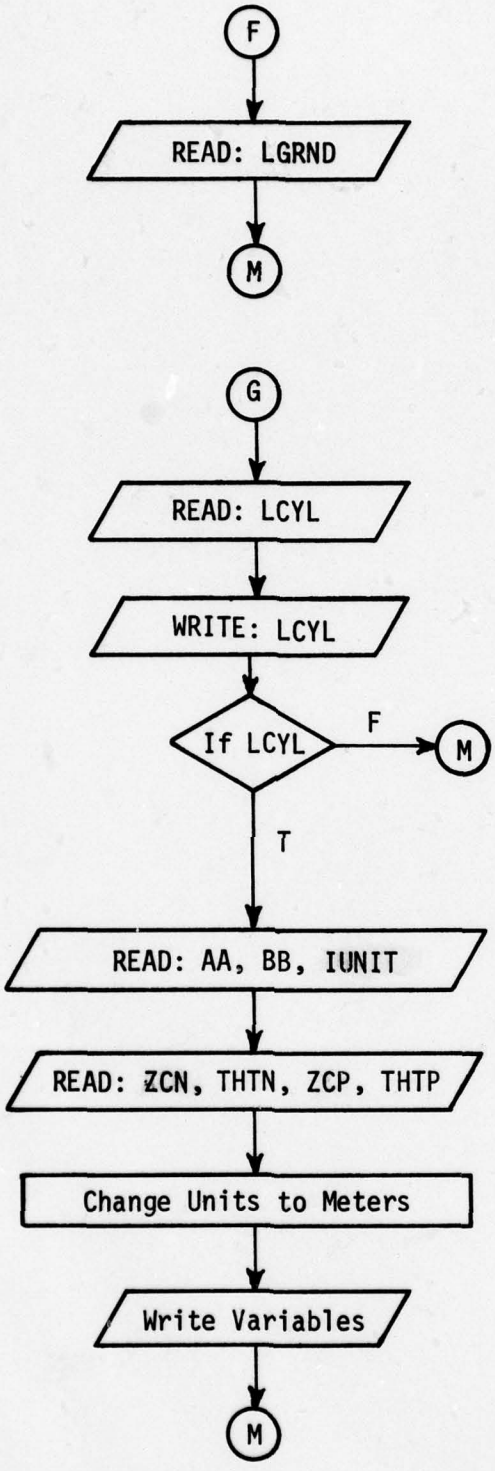
F
READ: LGRND
M
G
READ: LCYL
WRITE: LCYL
If LCYL
F
M
T
READ: AA, BB, IUNIT
READ: ZCN, THTN, ZCP, THTP
Change Units to Meters
Write Variables
M

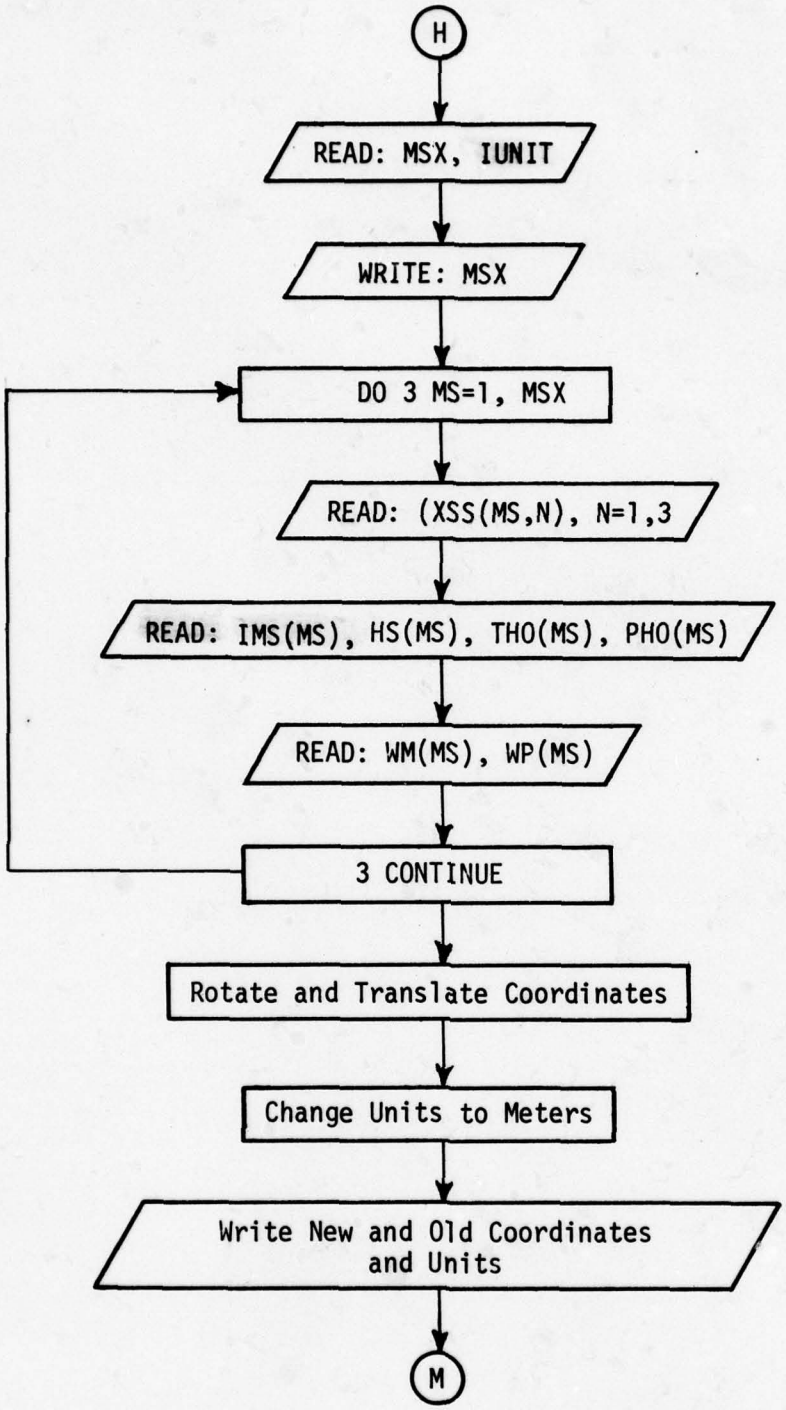
H
READ: MSX, IUNIT
WRITE: MSX
DO 3 MS=1, MSX
READ: (XSS(MS,N), N=1,3
READ: IMS(MS), HS(MS), THO(MS), PHO(MS)
READ: WM(MS), WP(MS)
3 CONTINUE
Rotate and Translate Coordinates
Change Units to Meters
Write New and Old Coordinates and Units
M

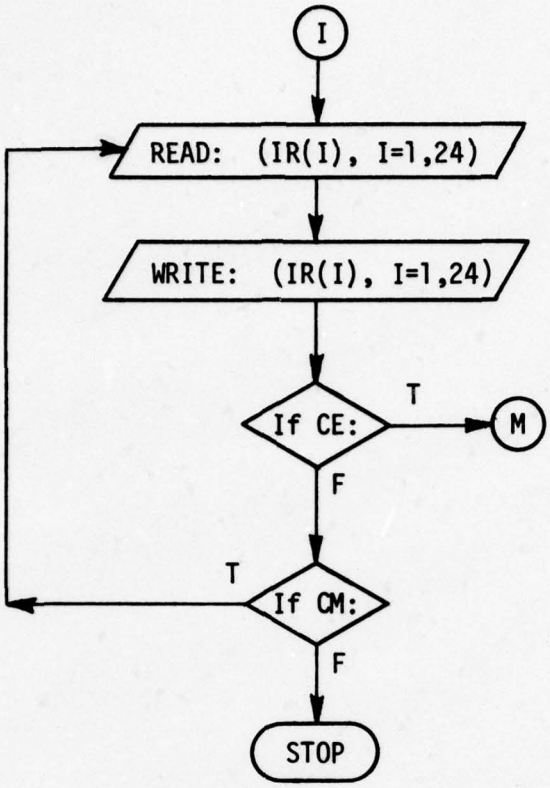
I
READ: (IR(I), I=1,24)
WRITE: (IR(I), I=1,24)
If CE:
T
M
F
T
If CM:
F
STOP

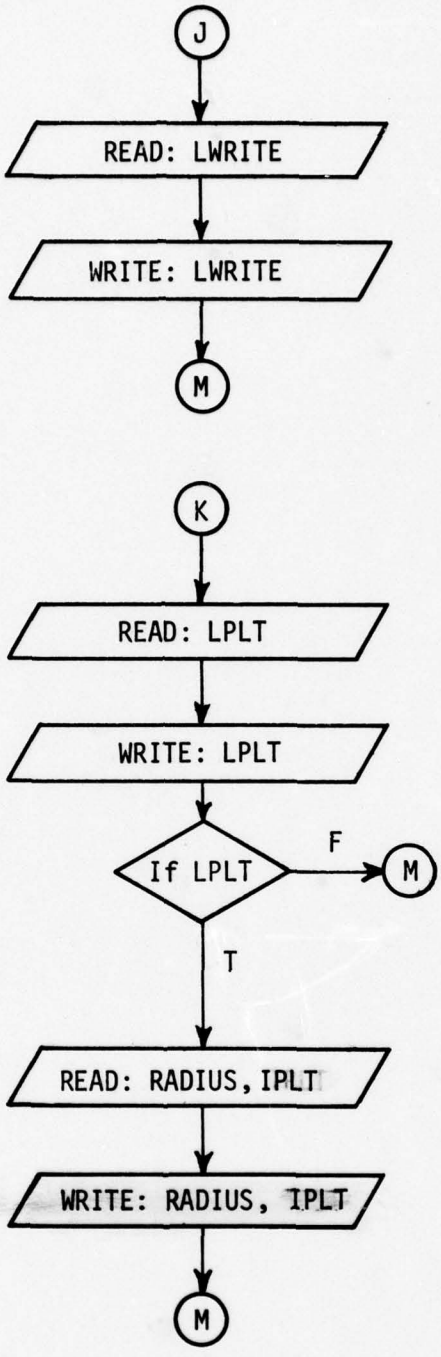
J
READ: LWRITE
WRITE: LWRITE
M
K
READ: LPLT
WRITE: LPLT
If LPLT
F
M
T
READ: RADIUS, IPLT
WRITE: RADIUS, IPLT
M

A. Command TO:

This command enables the user to obtain an extended output of various intermediate quantities in the computer code. This is useful in testing the program or in analyzing the contributions from various scattering mechanisms in terms of the total solution.

1. READ: LDEBUG, LTEST, LOUT

   a) LDEBUG: This is a logical variable defined by T or F. It is used to debug the program if errors are suspected within the program. If set true, the program prints out data on unit #6 associated with each of its internal operations. These data can, then, be compared with previous data which are known to be correct. It is, also, used to insure initial operation of the code. Only one pattern angle is considered. (normally set false)

   b) LTEST: This is a logical variable defined by T or F. It is used to test the input/output associated with each subroutine. The data written out on unit #6 are associated with the data in the window of the subroutine. They are written out each time the subroutine is called. It is, also, used to insure initial operation of the code. Only one pattern angle is considered. (normally set false)

   c) LOUT: This is a logical variable defined by T or F. It is used to output data on unit #6 associated with the main program. It too is used to initially insure proper operation. It can be used to examine the various components of the pattern. (normally set false)

2. READ: LSLOPE, LCORNR, LSOR

   a) LSLOPE: This is a logical variable defined by T or F. It is used to tell the code whether or not slope diffraction is desired during the computation. (normally set true)

   b) LCORNR: This is a logical variable defined by T or F. It is used to tell the code whether or not corner diffraction is desired during the computation. (normally set true)

c) LSOR: This is a logical variable which is defined by T or F. It is used to specify whether or not the operator wants simply the antenna pattern alone.(normally set false)

3. READ: JMN(1), JMX(1), JMN(2), JMX(2), JMN(3), JMX(3)

a) JMN(1), JMX(1): These are integer variables used to specify a set of individual scattering components that are to be included in the scattered field computation for the plate structures alone. JMN(1) is the minimum component number and JMX(1) is the maximum component number for the range of the set where the components are defined by the following number designations:
1 = incident field
2 = single reflected fields
3 = double reflected fields
4 = single diffracted fields
5 = reflected-diffracted fields
6 = diffracted-reflected fields
7 = identifies double diffracted problem areas (double diffracted fields are not computed at present).
Normally JMN(1)=1 and JMX(1)=7. This would compute all the available field values for a convex or concave plate structure.

b) JMN(2), JMX(2): These are integer variables used to specify a set of individual scattering components that are to be included in the scattered field computation for the finite elliptic cylinder structure alone. JMN(2) is the minimum component number and JMX(2) is the maximum component number for the range of the set where the components are defined by the following number designations:
1 = incident, reflected, transition and creeping wave fields.
2 = single reflected fields from the end caps.
3 = single diffracted fields from the end cap rims.
Normally JMN(2)=1 and JMX(2)=3.
This would compute all the field values for a finite elliptic cylinder structure.

c) JMN(3), JMX(3): These are integer variables used to specify a set of individual scattering components that are to be included in the scattered field computation for the interactions between the plate and cylinder structures. JMN(3) is the minimum component number and JMX(3) is the maximum component number for the range of the set where the components are defined by the following number designations:

1 = fields reflected from the plates then reflected or diffracted from the cylinder.

2 = fields reflected from the cylinder then reflected from the plates.

3 = fields reflected from the cylinder then diffracted from the plates.

4 = fields diffracted from the plates then reflected from the cylinder.

Normally JMN(3)=1 and JMX(3)=4.

B. Command PD:

This command enables the user to define the pattern axis of rotation, the angular range, and the frequency.

1. READ: THC, PHC, THP

This set of data is associated with the conical pattern desired during execution of the program. The pattern axis is defined by the spherical angles (THC, PHC) as illustrated in Figure 1. These angles define a radial vector direction which points in the direction of the pattern axis of rotation. These angles actually set-up a new coordinate system in relation to the original fixed coordinates. The new cartesian coordinates defined by the subscript "p" are found by first rotating about the z-axis the angle PHC and, then, about the y_p-axis the angle THC. The pattern is, then, taken in the "p" coordinate system in terms of spherical angles. The theta angle of the pattern taken about the z_p-axis is defined by THP. The phi angle is defined by the next read statement. In the present form the program will, then, compute any conical pattern in that THP is used as the conical pattern angle about the z_p-axis for the complete pattern calculation.

As an aid in setting up the "p" coordinate system the following set of equations give the relationships between (THC, PHC) and the x_p, y_p, z_p-axes. Note that the "p" axes are defined as radial vector directions in the spherical coordinate system:

$$\hat{x}_p = \cos(PHC)\sin(THC+90°)\hat{x}+\sin(PHC)\sin(THC+90°)\hat{y} + \cos(THC+90°)\hat{z}$$

$$\hat{y}_p = \cos(PHC+90°)\hat{x} + \sin(PHC+90°)\hat{y}$$

$$\hat{z}_p = \cos(PHC)\sin(THC)\hat{x} + \sin(PHC)\sin(THC)\hat{y} + \cos(THC)\hat{z}$$

where $0 \leq THC \leq 180°$ and $0 \leq PHC \leq 360°$. In its present form it should be noted that the user may not be able to define the x_p-axis at the starting location that he desires. In addition, the rotation of the pattern may be in the opposite sense using this approach. However, these problems can be easily overcome with properly written plot routines.

a) THC, PHC: These are real variables. They are input in degrees and define the axis of rotation about which a conical pattern will be computed.

b) THP: This is a real variable. It is input in degrees and used to define the conical angle about the axis of rotation for the desired pattern.

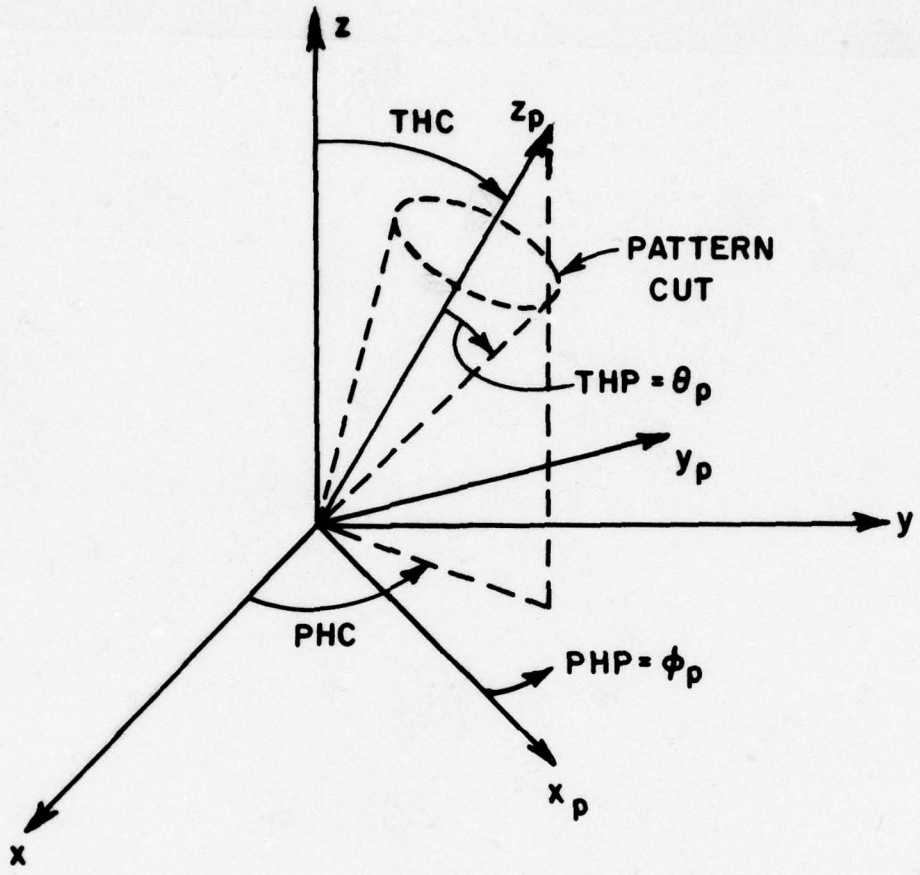

Figure 1. Definition of pattern axis.

2. READ: IB, IE, IS

a) IB, IE, IS: These are integer variables used to define angles in degrees. They are, respectively, the beginning, ending, and incremental values of the phi pattern angle.

As a result of the input given by the two previous read statements, the operator has completely defined the desired conical pattern to be computed during execution of the program.

3. READ: FRQG

a) FRQG: This is a real variable which is used to define the frequency in gigahertz.

C. Command RG:

This command enables the user to specify a far field distance, R, to the observer. The fields are then normalized by the factor exp(-jkR)/R.

1. READ: LRANG

a) LRANG: This is a logical variable defined by T or F. If set true it enables a far field range to be specified. If set false the next read statement is skipped.

2. READ: RANGS, IUNIT

a) This is a real variable which is used to specify the far field range, R.

b) IUNIT: This is an integer variable that indicates the units for the input data that follows, such that if

$$\text{IUNIT} = \begin{cases} 1 \rightarrow \text{meters} \\ 2 \rightarrow \text{feet} \\ 3 \rightarrow \text{inches} \end{cases}$$

Note that R should be in the far field of the scattering structure, that is, $R > 2D^2/\lambda$ where D is the maximum dimension of the structure.

D. Command RT:

This command enables the user to translate and/or rotate the coordinate system used to define the input data in order to simplify the specification of the plate, cylinder, and source geometries. The geometry is illustrated in Figure 2.

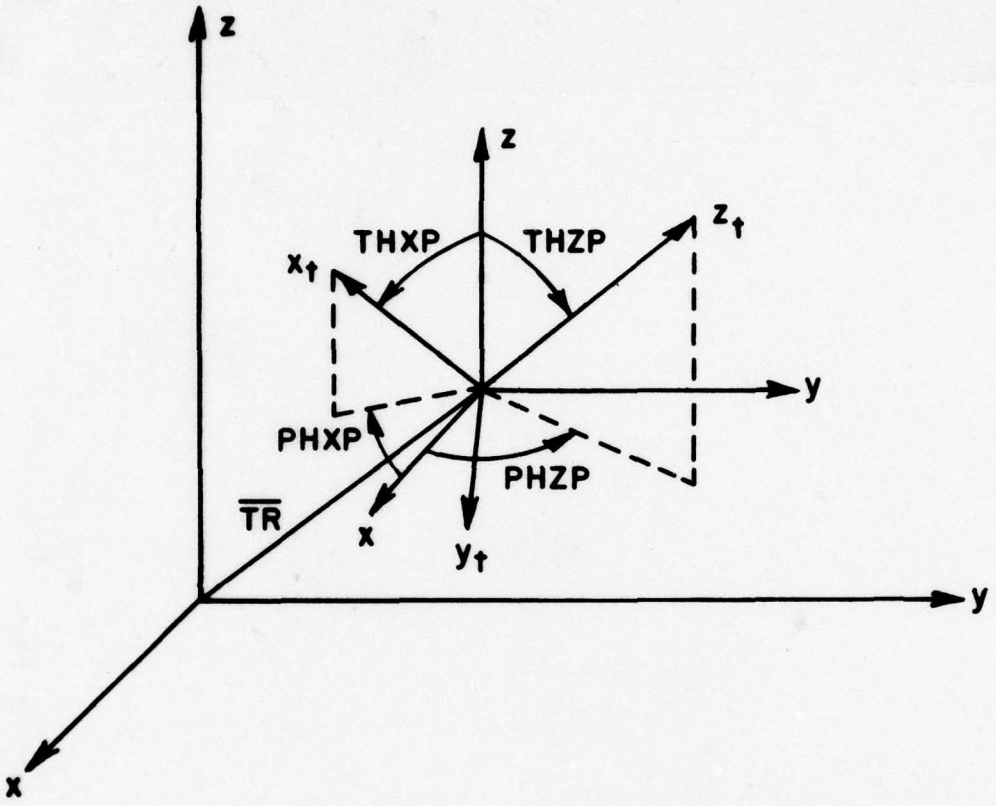

Figure 2. Definition of rotate-translate coordinate system geometry.

1. READ: IUNIT, (TR(N), N=1,3)

   a) IUNIT: This is an integer variable that indicates the units for the input data that follows, such that

   $$IUNIT = \begin{cases} 1 \rightarrow \text{meters} \\ 2 \rightarrow \text{feet} \\ 3 \rightarrow \text{inches} \end{cases}$$

   b) TR(N): This is a dimensional real variable. It is used to specify the origin of the new coordinate system to be used to input the data for the source or the scattering structures. It is input on a single line with the real numbers being the x,y,z coordinates of the new origin which corresponds to N=1,2,3, respectively.

2. READ: THZP, PHZP, THXP, PHXP

a) THZP, PHZP: These are real variables. They are input in degrees as spherical angles that define the z-axis of the new coordinate system as if it was a radial vector in the reference coordinate system.

b) THXP, PHXP: These are real variables. They are input in degrees as spherical angles that define the x-axis of the new coordinate system as if it was a radial vector in the reference coordinate system.

The new x-axis and z-axis must be defined orthogonal to each other. The new y-axis is found from the cross product of the x and z axes. All the subsequent inputs will be made relative to this new coordinate system, which is shown as x_t, y_t, z_t, unless command "RT:" is called again and redefined.

E. Command PG:

This command enables the user to define the geometry of the flat plate structures to be considered. The geometry is illustrated in Figure 3.

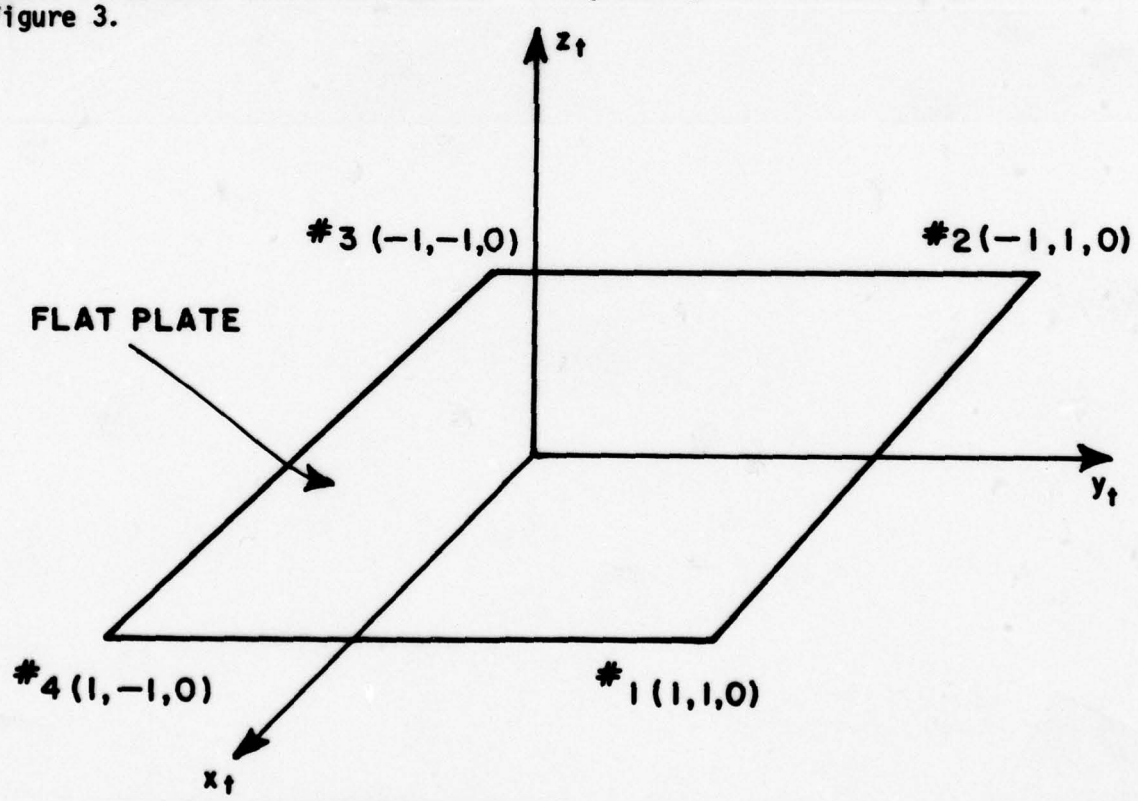

Figure 3. Definition of flat plate geometry.

1. READ: LPLA

   a) LPLA: This is a logical variable defined by T or F. It is used to specify whether or not there will be any plate scattering structures defined. IF LPLA is false the rest of the READ statements for this command will be skipped.

2. READ: MPX, IUNIT

   a) MPX: This is an integer variable which defines the maximum number of plates to be used in the present simulation of the structure. Presently, $1 \leq MPX \leq 14$.

   b) IUNIT: This is an integer variable that indicates the units for the input data that follows, such that if

$$IUNIT = \begin{cases} 1 \rightarrow \text{meters} \\ 2 \rightarrow \text{feet} \\ 3 \rightarrow \text{inches} \end{cases}$$

3. READ: (MEP(MP), MP=1, MPX)

   a) MEP (MP): This is a dimensioned integer variable. It is used to define the number of corners (or edges) on the MP^{th} plate. They are defined on the same data line with commas between integer values. Presently, $1 \leq MEP(MP) \leq 6$ with $1 \leq MP \leq 14$.

4. READ: (XX(MP,ME,N), N=1,3)

As stated earlier the locations of the corners of the flat plates are input in terms of the x, y, z coordinates in the specified cartesian coordinate system.

   a) XX(MP,ME,N): This is a triply dimensioned real variable. It is used to specify the location of the ME^{th} corner of the MP^{th} plate. It is input on a single line with the real numbers being the x,y,z coordinates of the corner which correspond to N=1,2,3, respectively, in the array. For example, the array will contain the following for plate #1 and corner #2 located at x=2., y=4., z=6.:
   x(1,2,1)=2.
   x(1,2,2)=4.
   x(1,2,3)=6.
   This data is input as: 2.,4.,6.

Considering the flat plate structure given in Figure 3, the input data is given by

```
 1., 1., 0                  : corner #1 }
-1., 1., 0.                 : corner #2 }
-1.,-1., 0.                 : corner #3 }   plate #1
 1.,-1., 0.                 : corner #4 }
```

Presently: $1 \leq MP \leq 14$
$1 \leq ME \leq 6$
$1 \leq N \leq 3$

(See Chapter IV for further details in defining the corner points.)

F. Command GP:

This command enables the user to specify a perfectly conducting infinite ground plane in the x-y plane.

1. READ: LGRND

a) LGRND: This is a logical variable which is defined by T or F. It is used to specify whether or not a perfectly conducting infinite ground plane is desired in the x-y plane (fixed coordinate system). If LGRND is set true the logical variable LPLA will automatically be set true since the ground plane is considered to be a very large plate for computation purposes.

G. Command CG:

This command enables the user to define the geometry of the finite elliptic cylinder structure to be considered. Note only one may be specified. The geometry is illustrated in Figure 4.

1. READ: LCYL

a) LCYL: This is a logical variable defined by T or F. It is used to specify whether or not there will be a cylinder defined. If LCYL is false the rest of the READ statements for this command will be skipped.

2. READ: AA, BB, IUNIT

a) AA: This is a real variable which defines the radius of the elliptic cylinder on the x-axis of the cylinder.

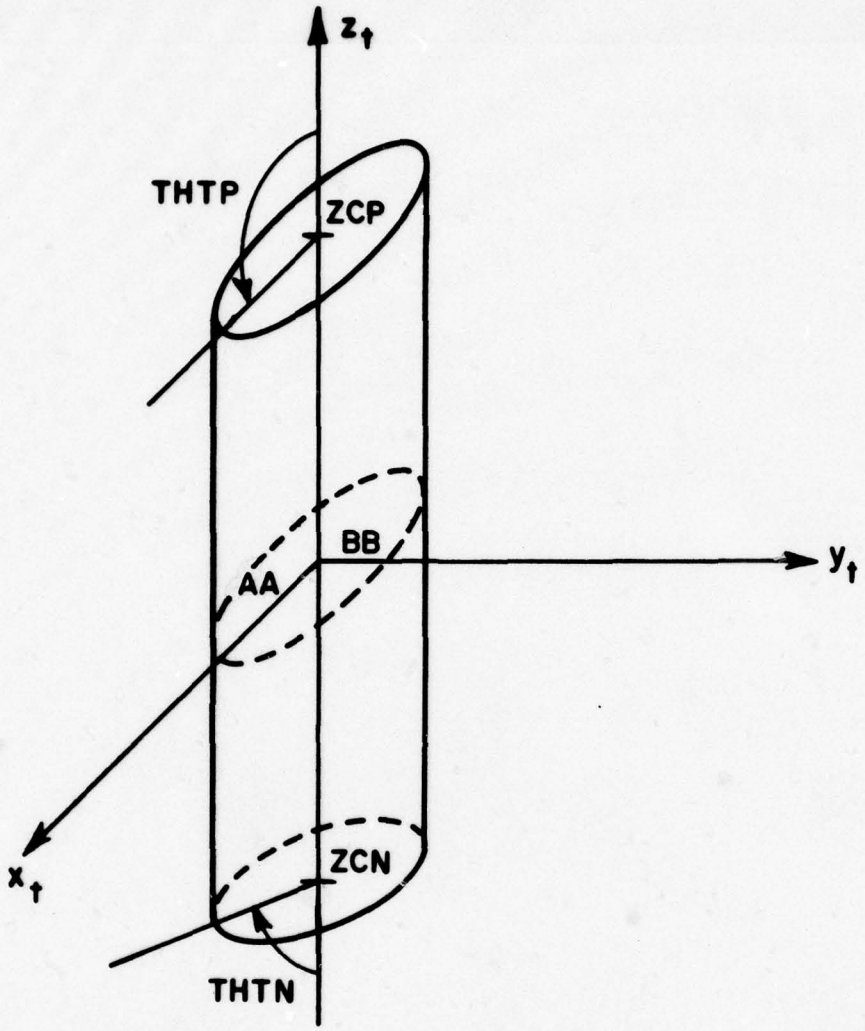

Figure 4. Definition of finite elliptic cylinder geometry.

b) BB: This is a real variable which defines the radius of the elliptic cylinder on the y-axis of the cylinder.

c) IUNIT: This is an integer variable that indicates the units for the input data that follows, such that if

$$IUNIT = \begin{cases} 1 \rightarrow \text{meters} \\ 2 \rightarrow \text{feet} \\ 3 \rightarrow \text{inches.} \end{cases}$$

3. READ: ZCN, THTN, ZCP, THTP

a) ZCN: This is a real variable that defines the position of the center of the most negative endcap on the z-axis of the cylinder.

b) THTN: This is a real variable. It is input in degrees and defines the angle the surface of the most negative endcap makes with the negative z-axis in the x_t-z_t plane.

c) ZCP: This is a real variable that defines the position of the center of the most positive endcap on the z-axis of the cylinder.

d) THTP: This is a real variable. It is input in degrees and defines the angle the surface of the most positive endcap makes with the positive z-axis in the x_t-z_t plane.

H. Command SG:

This command enables the user to specify the location and type of source to be used. The geometry is illustrated in Figure 5.

1. READ: MSX, IUNIT

a) MSX: This is an integer variable which defines the maximum number of elemental radiators to be considered during execution of the program. Presently, $1 \leq MSX \leq 50$.

b) IUNIT: This is an integer variable that indicates the units for the input data that follows, such that if

$$IUNIT = \begin{cases} 1 \rightarrow \text{meters} \\ 2 \rightarrow \text{feet} \\ 3 \rightarrow \text{inches} \end{cases}$$

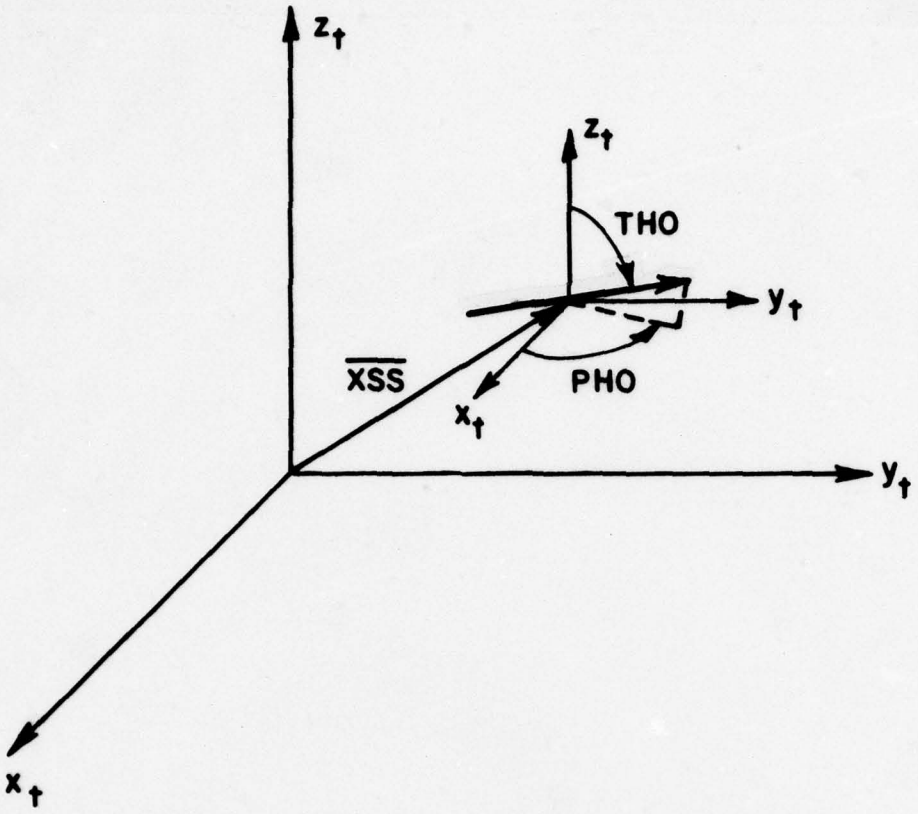

Figure 5. Definition of source geometry.

2. READ: (XSS (MS,N) N=1,3)

   a) XSS (MS,N): This is a doubly dimensioned real array which is used to define the x,y,z location of the MSth *elemental* radiator in the specified cartesian coordinate system. Again, a single line of data contains the x,y,z (N=1,2,3) locations. Presently, $1 \leq MS \leq 50$
   $1 \leq N \leq 3$

(See Chapter IV for further details on defining the source point.)

3. READ: IMS(MS), HS (MS), THO (MS), PHO (MS)

a) IMS (MS): This is an integer array which is used to define whether the MS^{th} source is an electric or magnetic elemental radiator.
IMS (MS) = 0 → electric
IMS (MS) = 1 → magnetic

b) HS (MS): This is a real array which is used to input the length of the MS^{th} element in electrical wavelengths. It is not input in inches.

c) THO (MS), PHO (MS): These are real arrays which are used to define the orientation of the MS^{th} element in the specified cartesian coordinate system. The THO, PHO angles are in degrees and define a radial direction which is parallel to the MS^{th} element current flow. Again, THO is the theta angle and PHO is the phi angle in a normal spherical coordinate system.
Presently, $1 \leq MS \leq 50$.

4. READ: WM (MS), WP (MS)

a) WM (MS), WP (MS): These are real dimensioned arrays used to define the excitation associated with the MS^{th} element. The magnitude is given by WM and the phase in degrees by WP.
Presently, $1 \leq MS \leq 50$.

I. Commands CM: and CE:

These commands enable the user to place comment cards in the input and output data in order to help identify the computer runs for present and future reference.

1. READ: (IR(I), I=1,24)

a) IR(I): This is an integer dimensioned array used to store the command word and comments. Each card should have CM: or CE: on them followed by an alphanumeric string of characters. The CM: command implies that there will be another comment card following it. The last comment card must have the CE: command on it. If there is only one comment card the CE: command must be used.
Note: It is possible to place comments to the right of all the command words, if desired.

J. Command LP:

This command enables the user to specify whether a line printer listing of the results is desired.

1. READ: LWRITE

   a) LWRITE: This is a logical variable defined by T or F. It is used to indicate if a line printer listing of the total fields ($E_{\theta p}$,$E_{\phi p}$) is desired. (normally set true)

K. Command PP:

1. READ: LPLT

   a) LPLT: This is a logical variable defined by T or F. It is used to indicate if a polar plot of the total fields ($E_{\theta p}$,$E_{\phi p}$) is desired. If LPLT is false the rest of the READ statements for this command will be skipped.

2. READ: RADIUS, IPLT

   a) RADIUS: This is a real variable that is used to specify the radius of the polar plot.

   b) IPLT: This is an integer variable that indicates the type of polar plot desired, such that if

$$\text{IPLT} = \begin{cases} 1 \rightarrow \text{field plot} \\ 2 \rightarrow \text{power plot} \\ 3 \rightarrow \text{dB plot} \end{cases}$$

The fields will be normalized by their maximum field values.

L. Command EX:

This command is used to execute the scattering code so that the total fields may be computed. After execution the code returns for another possible command word.

This concludes the definition of all the input parameters to the program. The program would, then, run the desired data and output the results on unit #6. However as with any sophisticated program, the definition of the input data is not sufficient for one to fully understand the operation of the code. In order to overcome this difficulty the next chapter discusses how the input data are interpreted and used in the program.

IV. INTERPRETATION OF INPUT DATA

This computer code is written to require a minimum amount of user information such that the burden associated with a complex geometry will be organized internal to the computer code. For example, the operator need not instruct the code that two plates are attached to form a convex or concave structure. The code flags this situation by recognizing that two plates have a common set of corners (i.e., a common edge). So if the operator wishes to attach two plates together he needs only define the two plates as though they were isolated. However, the two plates will have two identical corners. All the geometry information associated with plates with common edges is then generated by the code. The present code also will allow a plate to intersect another plate as shown in Figure 6. It is necessary that the corners defining the attachment be positioned a small amount (approximately 10^{-6} wavelengths) through the plate surface to which it is being connected.

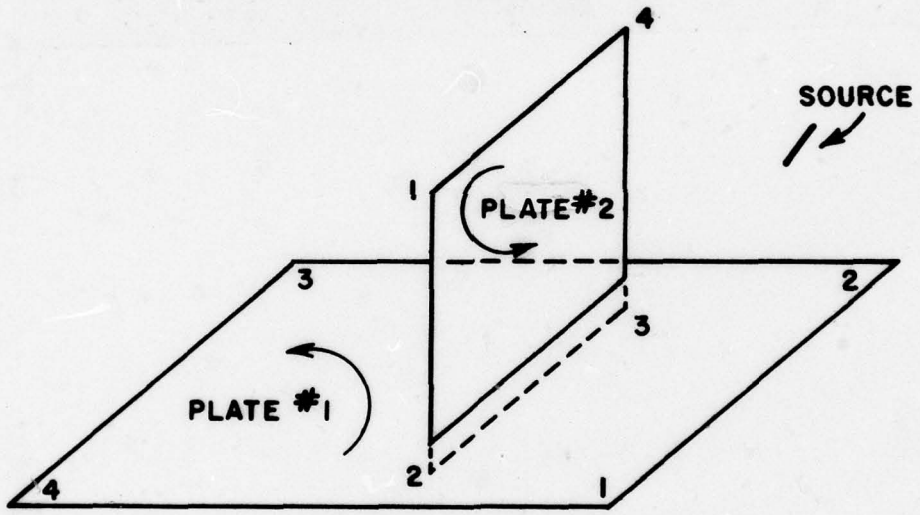

Figure 6. Data format used to define a flat plate intersecting another flat plate.

In defining the plate corners it is necessary to be aware of a subtlety associated with simulating convex or concave structures in which two or more plates are used in the computation. This problem results in that each plate has two sides. If the plates are used to simulate a closed or semi-closed structure, then possibly only one

side of the plate will be illuminated by the antenna. Consequently, the operator must define the data in such a way that the code can infer which side of the plate is illuminated by the antenna. This is accomplished by defining the plate according to the right-hand rule. As one's fingers of the right hand follow the edges of the plate around in the order of their definition, his thumb should point toward the illuminated region above the plate. To illustrate this constraint associated with data format, let us consider the definition of a rectangular box. In this case, all the plates of the box must be specified such that they satisfy the right-hand rule with the thumb pointing outward as illustrated in Figure 7. If this rule were not satisfied for a given plate, then the code would assume that the antenna is within the box as far as the scattering from that plate is concerned.

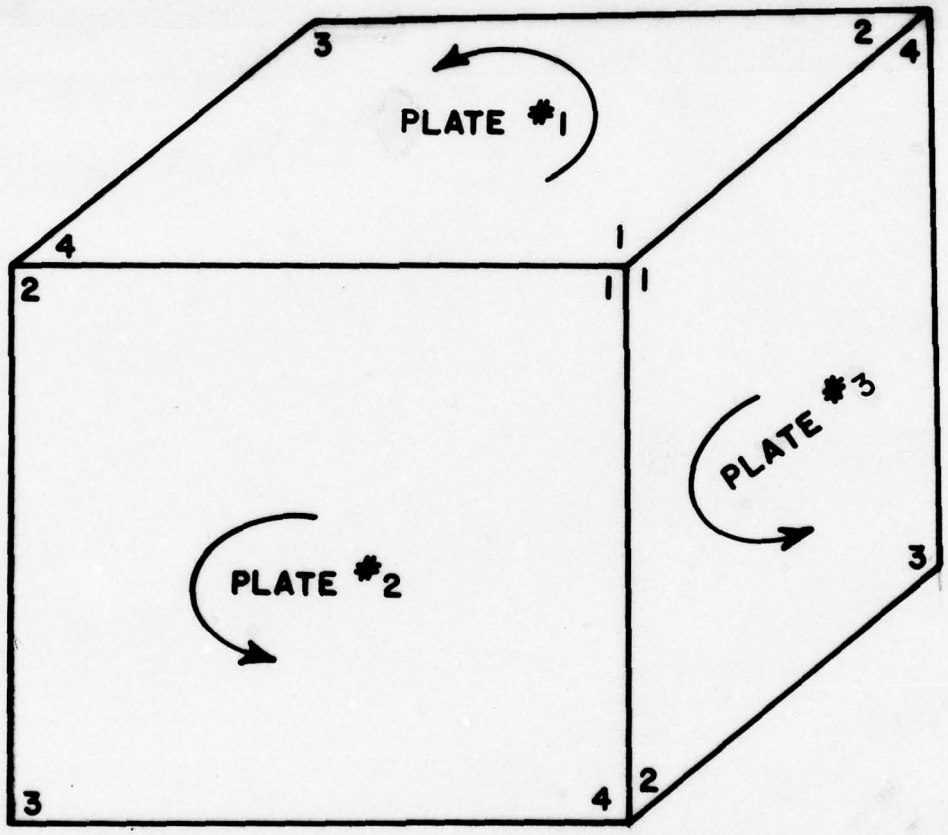

Figure 7. Data format used to define a box structure.

Another situation which must be kept in mind is associated with antenna elements mounted on a plate. The code automatically determines that the antenna element is mounted on the plate. It assumes that the element will radiate on the side of the plate into which the normal points. This is accomplished in the code by automatically positioning the source a small distance (10^{-6} wavelengths above the plate in the direction of the normal as illustrated in Figure 8. It is important,

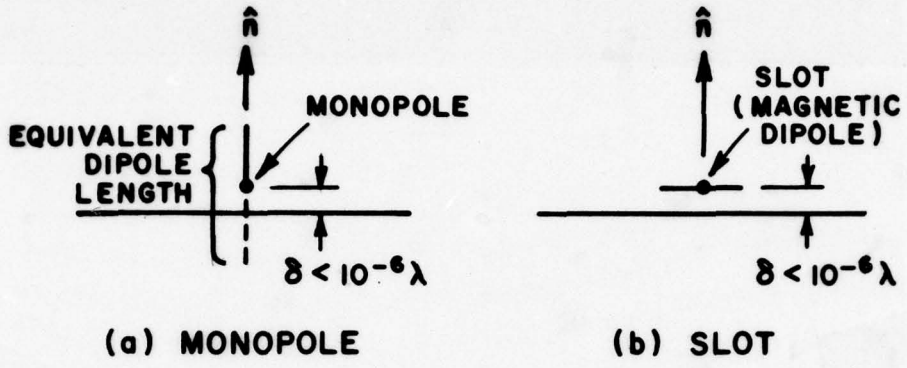

Figure 8. Illustration of geometry for plate-mounted antennas.

therefore, to follow the simple rules above for defining the plate normals when dealing with plate mounted antennas. There is, also, another point associated with antennas mounted on perfectly-conducting flat structures. If a plate-mounted monopole is considered in the computation, one should input the equivalent dipole length and not the monopole length (i.e., the monopole plus image length should be used as shown in Figure 8a). The code automatically handles the half dipole modes associated with the monopole. The plate-mounted slot is, also, automatically taken care of by the code as shown in Figure 8b if a magnetic dipole is used.

The same situation arises when the antenna is mounted on the elliptic cylinder's end caps. It should also be remembered that the antenna can not be mounted on the curved part of the cylinder. In general, the antenna should be kept a wavelength away, however, this can often be relaxed to approximately a quarter-wavelength.

In the present code, the attachment of a plate corner to the curved surface of the cylinder is automatically detected, however, a diffracted field from the plate-cylinder junction is not considered in this version. If the plate-cylinder junction forms a straight, orthogonal edge, as shown in the aircraft models of Figures 22 and 24, image theory alone will give the correct results. The diffracted fields, therefore, are not needed. If the plate-cylinder junction forms a curved edge or one

in which the plate and cylinder surface are not orthogonal a diffracted field from that edge will be required in the solution. This will be added when time and effort permit.

Section VI has a set of sample problems to illustrate how the operator can realize the versatility of the code and still satisfy the few constraints associated with the input data format.

V. INTERPRETATION OF OUTPUT

The basic output from the computer code is a line printer listing of the results. The results are referenced to the pattern coordinate system that was described in Section IV and is illustrated in Figure 1. Thus the total electric field is given by

$$\bar{E}(\theta_p,\phi_p) = \hat{\theta}_p E_{\theta p} + \hat{\phi}_p E_{\phi p}.$$

The fields are assumed to be peak values given in volts/unit when the factor e^{-jkR}/R is suppressed in the far field. If an R value is specified using the "RG:" command then the results will be in volts/meter. The results are displayed in three sections. The first output associated with the $E_{\theta p}$ field, the second is output associated with the $E_{\phi p}$ field, and the third is output associated with the total field. The first section is displayed as follows: θ_p, ϕ_p, $E_{\theta p}$, $\underline{/E_{\theta p}}$ (phase of $E_{\theta p}$), $|E_{\theta p}|$ (magnitude of $E_{\theta p}$), $G_{d\theta}$ (directive gain $E_{\theta p}$), $|E_{\theta p}|/|E_{\theta p}|_{max}$ (normalized magnitude of $E_{\theta p}$), $G_{d\ norm}$ (normalized value of the directive gain). The second section is similarly done for the $E_{\phi p}$ field. The third section is displayed as follows: θ_p, ϕ_p, $G_{d\ major}$ (directive gain of E_{major}), $G_{d\ minor}$ (directive gain of E_{minor}), γ (tilt angle of polarization ellipse, axial ratio, G_d (total directive gain), $G_{d\ norm}$ (normalized total directive gain). The above quantities are defined as follows:

$$G_d = \frac{2\pi R^2}{\eta_o P_{rad}} \bar{E} \cdot \bar{E}^* ,$$

$$G_{d\theta} = \frac{2\pi R^2}{\eta_o P_{rad}} |E_{\theta p}|^2 ,$$

$$G_{d\phi} = \frac{2\pi R^2}{\eta_o P_{rad}} |E_{\phi p}|^2 ,$$

$$G_{d\ major} = \frac{2\pi R^2}{\eta_o P_{rad}} |E_{major}|^2 ,$$

$$G_{d\ minor} = \frac{2\pi R^2}{\eta_o P_{rad}} |E_{minor}|^2 ,$$

$$E_{major} = [(|E_{\theta p}|\cos\gamma + |E_{\phi p}|\cos\psi\sin\gamma)^2 + |E_{\phi p}|^2 \sin^2\psi\sin^2\gamma]^{1/2} ,$$

$$E_{minor} = [(|E_{\theta p}|\sin\gamma - |E_{\phi p}|\cos\psi\cos\gamma)^2 + |E_{\phi p}|^2 \sin^2\psi\cos^2\gamma]^{1/2},$$

$$\psi = \underline{/E_{\phi p}} - \underline{/E_{\theta p}} , \qquad [10,11]$$

$$\gamma = \frac{1}{2} \tan^{-1} \left(\frac{2|E_{\theta p}||E_{\phi p}|\cos\psi}{|E_{\theta p}|^2 - |E_{\phi p}|^2} \right)$$

$$\text{axial ratio} = \left| \frac{E_{minor}}{E_{major}} \right|$$

η_o = free space impedance.

The value P_{rad} is the power radiated. The code makes a simple estimate of the power radiated based on isolated dipoles in free space. This is only meant to give a ball-park figure for the directive gain. It should be cautioned that this could be a rather crude estimate of the gain in any given situation. If a better estimate of the power radiated can be obtained, for example, from a moment method code, then that value could be used in the code to give a more accurate value for the directive gain.

A very convenient means of displaying the results of the program is through a polar plot representation. However, because of the difficulty of delivering standard plot routines from one computer system to another, our plot package is not included as an integral part of this computer code. A simple polar plot routine is given in Appendix I which can be used if desired. The proper subroutine for the particular computer used must be observed if the subroutine is to compile and execute as desired.

The next section displays the results in either polar or rectangular dB plots to compare against measured results whenever possible. The results are normalized to either 0 dB or the measured patterns maximum.

VI. APPLICATION OF CODE TO SEVERAL EXAMPLES

The following nine examples are used to illustrate the various features of the computer code. The results are presented in terms of polar and rectangular plots. The polar plots can be generated using the polar plot routine given in Appendix I. Note that the patterns are plotted in decibels with each division being 10 dB. The routine in Appendix I does not make any reference to a symbol subroutine, in that they are very much machine dependent. Thus, labeling is not included on the plots.

Note that the input data lists are shown containing most all of the commands needed for the particular examples given. In many cases the input list can be shortened because the data contained in the default list at the beginning of the program need not be input through the read statements every time. For example, the "TO:" command data could be left out of the input list in most of the examples given here. The user should refer to that section of the particular code that he is using to see what the defaults are. The default list can be changed to meet his particular needs if necessary.

Example 1. Consider the pattern of an electric dipole in the presence of a finite ground plane as shown in Figure 9. The input data is given by

```
TO:
F,F,F
T,T,F
1,7,1,3,1,4
PD:
0.,0.,90.
0,360,1
10.43
```

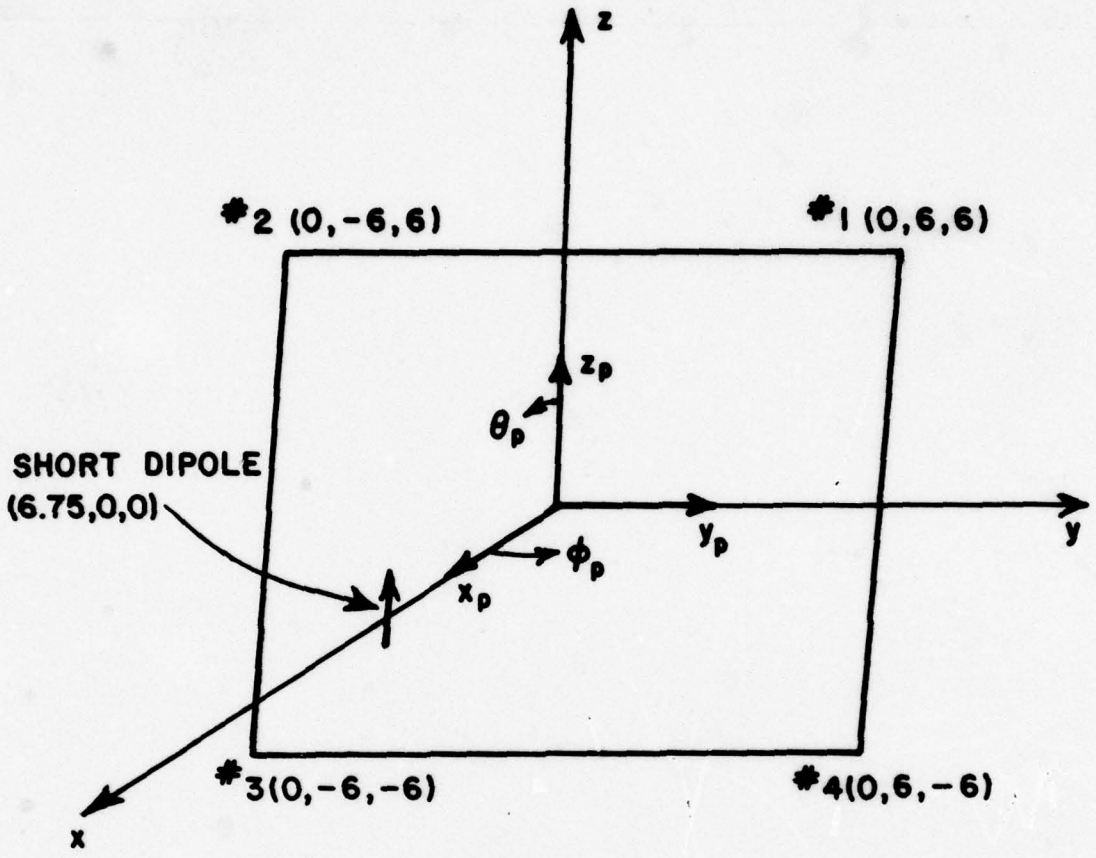

Figure 9. Short dipole in presence of a square ground plane.

```
PG:
T
1,3
4
0.,6.,6.    : corner #1 ┐
0.,-6.,6.   : corner #2 ├  Plate #1
0.,-6,-6.   : corner #3 ┤
0.,6.,-6.   : corner #4 ┘
SG:
1,3
6.75,0.,0.
0,.1,0.,0.
1., 0.
EX:
```

The $E_{\theta p}$ pattern is plotted in Figure 10. The $E_{\phi p}$ pattern is not plotted because it is of negligible value.

Example 2: Consider the pattern of a $\lambda/2$ slot antenna mounted in the center of a square ground plane as shown in Figure 11. The input data is given by:

```
PD:
90.,135.,90.
0,360,1
10.
PG:
T
1,3
4
6.,6.,0.
-6.,6.,0.
-6.,-6.,0.
6.,-6.,0.
```

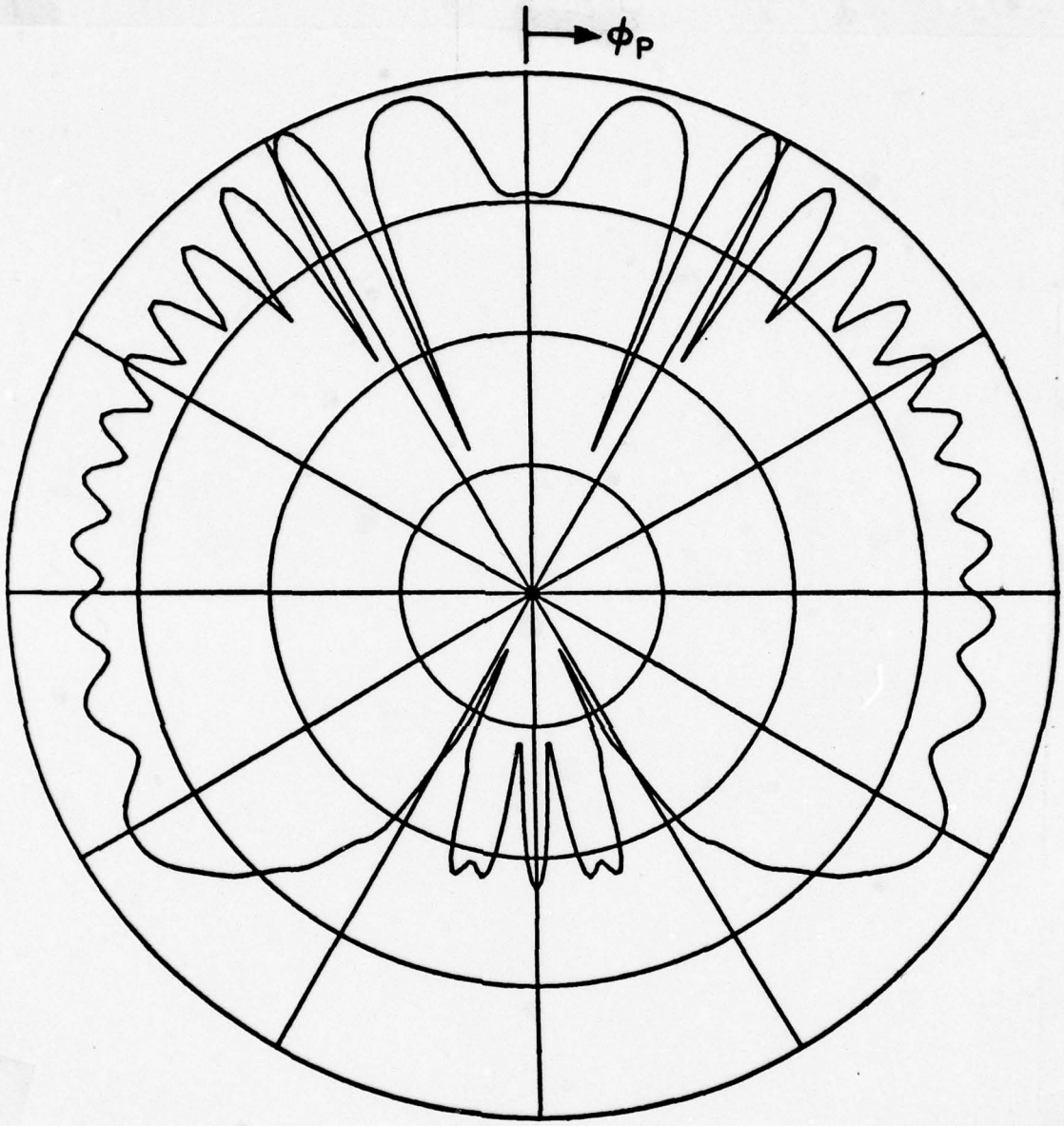

Figure 10. $E_{\theta P}$ radiation pattern for a short electric dipole located above a square plate at a frequency of 10.43 GHz.

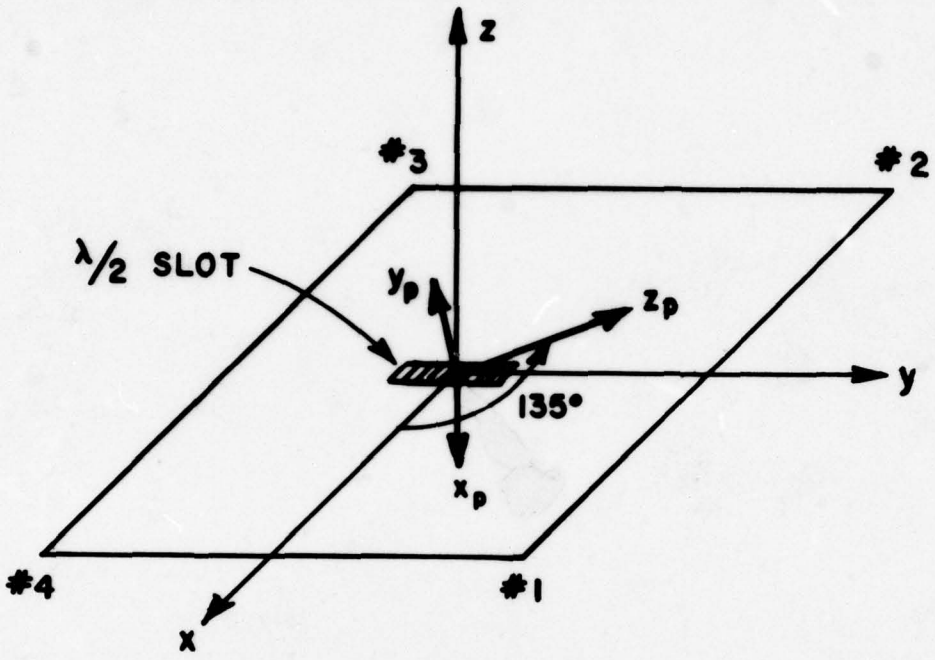

Figure 11. A λ/2 slot mounted on top of a square ground plane.

```
SG:
1,3
0.,0.,0.
1,.5,90.,90.
1.,0.
EX:
```

The E_{θ_p} and $E_{\phi p}$ patterns are plotted in Figure 12. Note this pattern is taken directly across the corner of the plate; yet, both patterns are continuous.

Example 3. Consider the pattern of an electric dipole in the presence of an eight-sided box as shown in Figure 13. The input data is given by:

```
PD:
0.,0.,90.
0,360,1
9.94
SG:
1,1
.212,0.,0.
0,0.5,0.,0.
1.,0.
PG:
T
8,1
4,4,4,4,4,4,6,6
.122,-.1023,-.1
.122,-.1023,.1
0.,-.1707,.1
0.,-.1707,-.1
.122,.1023,-.1
.122,.1023,.1
.122,-.1023,.1
.122,-.1023,-.1
0.,.1707,-.1
0.,.1707,.1
.122,.1023,.1
.122,.1023,-.1
-.122,.1023,-.1
-.122,1023,.1
0.,.1707,.1
```

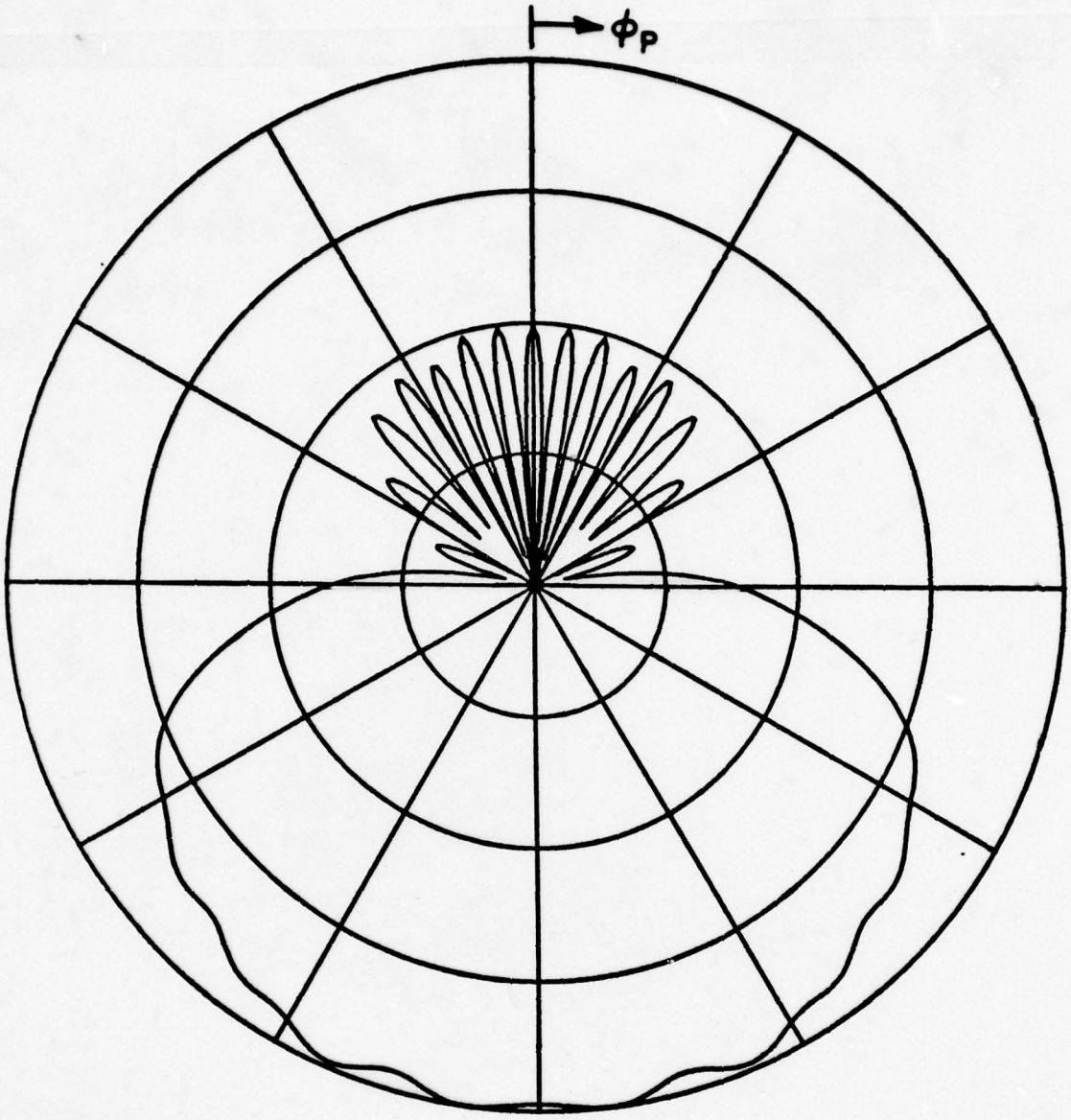

Figure 12a. $E_{\theta p}$ radiation pattern of $\lambda/2$ slot antenna mounted on a square ground plane at a frequency of 10 GHz.

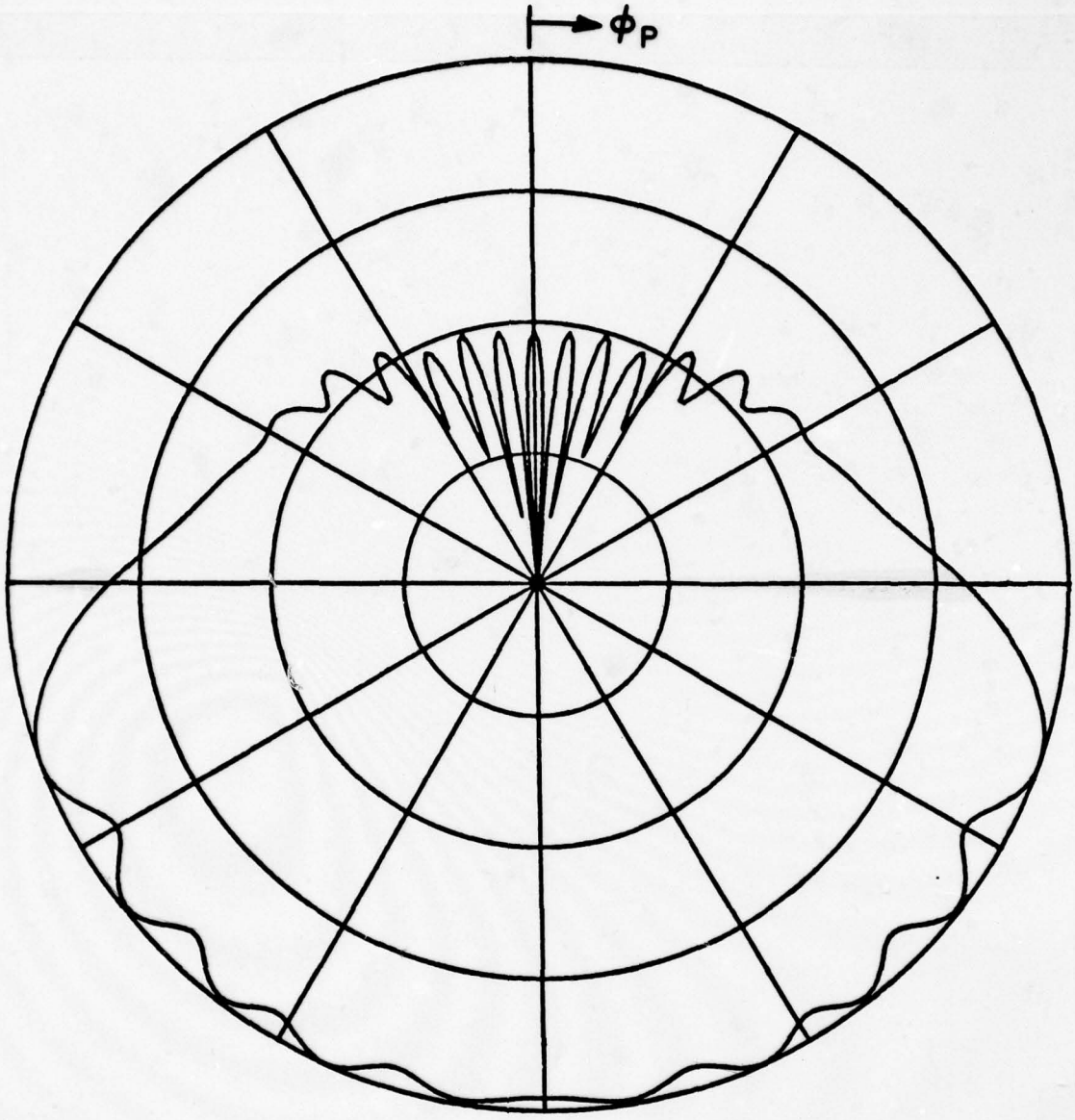

Figure 12b. $E_{\phi P}$ radiation pattern of $\lambda/2$ slot antenna mounted on a square ground plane at a frequency of 10 GHz.

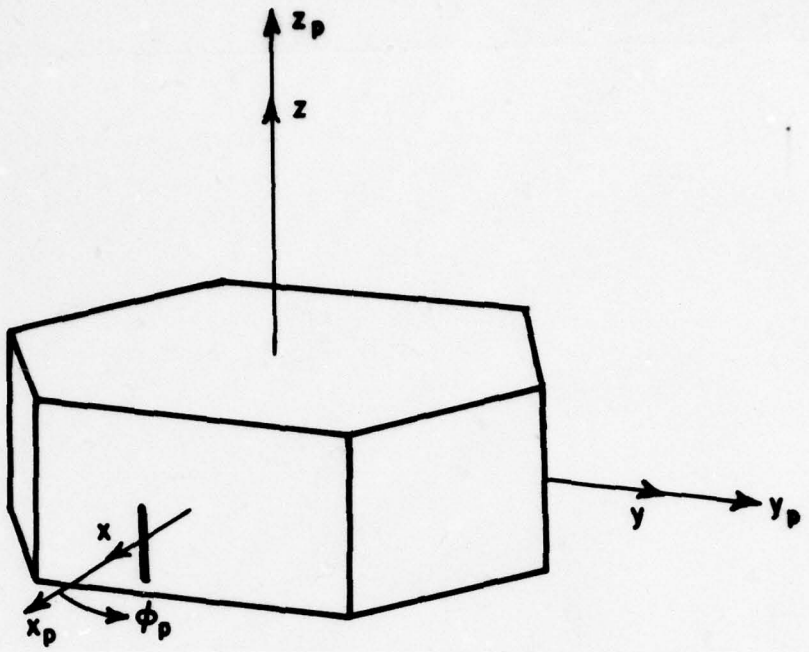

Figure 13. Electric dipole in the presence of an eight sided box.

```
0.,.1707,-.1
-.122,-.1023,-.1
-.122,-.1023,.1
-.122,.1023,.1
-.122,.1023,-.1
0.,-.1707,-.1
0.,-.1707,.1
-.122,-.1023,.1
-.122,-.1023,-.1
0.,.1707,.1
-.122,.1023,.1
-.122,-.1023,.1
0.,-.1707,.1
.122,-.1023,.1
.122,.1023,.1
0.,.1707,-.1
.122,.1023,-.1
.122,-.1023,-.1
0.,-.1707,-.1
-.122,-.1023,-.1
-.122,.1023,-.1
EX:
```

The $E_{\theta p}$ pattern is compared with measured results [12] in Figure 14. The $E_{\phi p}$ pattern is not plotted because it is of negligible value.

Example 4. Consider an electric dipole in the presence of a finite circular cylinder as shown in Figure 15. This example shows how once the cylinder geometry is set up different cases can be run by just changing the data that needs to be changed for the particular case to be run.

```
PD:
0.,0.,90.
0,360,1
9.94
SG:
1,1
0.,0.19,0.
0,0.5,90.,0.
1.,0.
CG:
T
0.1,0.1,1
-0.11,90.,0.11,90.
EX:
```

4a. original problem (Figure 15a)

```
PD:
90.,0.,90.
0,360,1
9.94
EX:
```

4b. pattern cut changed (Figure 15b)

```
SG:
1,1
0.076,0.0,0.2
0,0.5,90.,0.
1.,0.
EX:
```

4c. source location changed (Figure 15c)

The calculated results are compared with measured results [12] in the following figures.

The $E_{\phi p}$ pattern for example 4a is shown in Figure 16a.
The $E_{\theta p}$ pattern for example 4b is shown in Figure 16b.
The $E_{\theta p}$ pattern for example 4c is shown in Figure 16c.

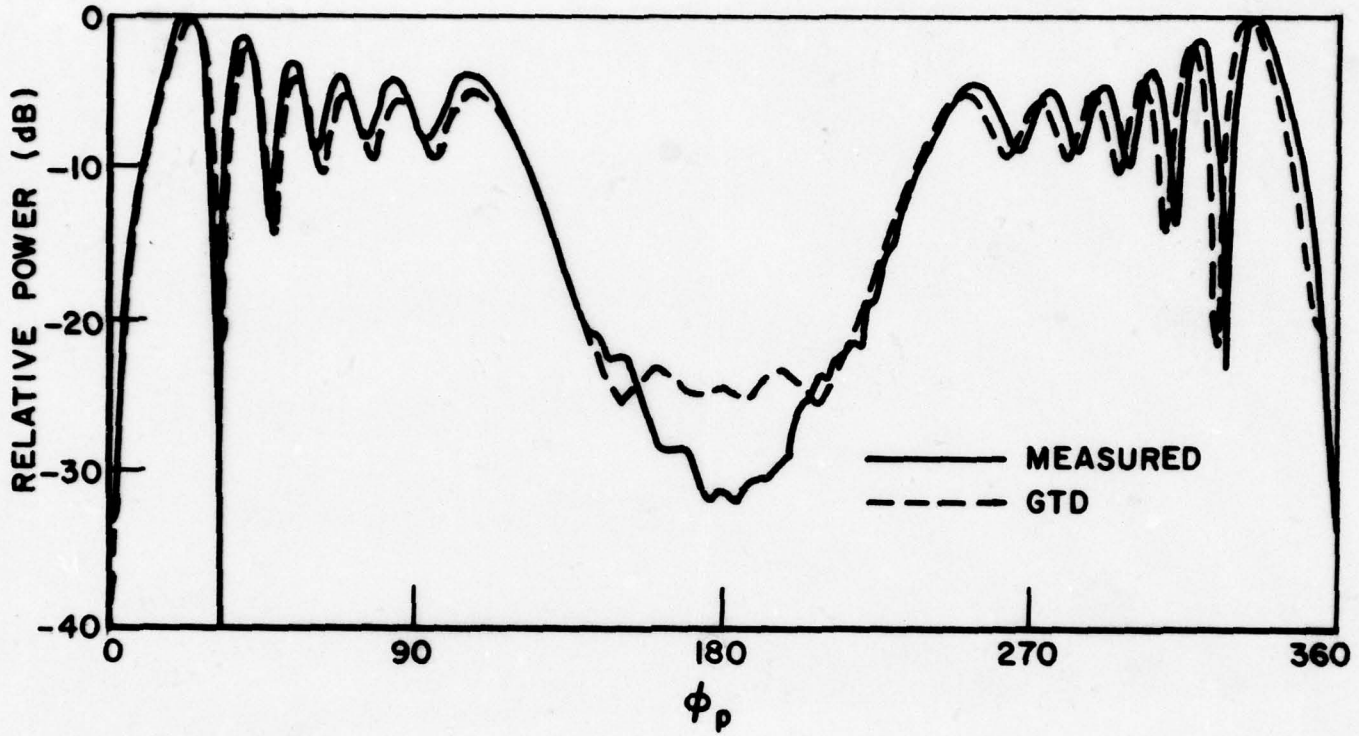

Figure 14. Comparison of measured (Bach) and calculated radiation pattern for E_{θ_p} for an electric dipole in the presence of an eight sided box.

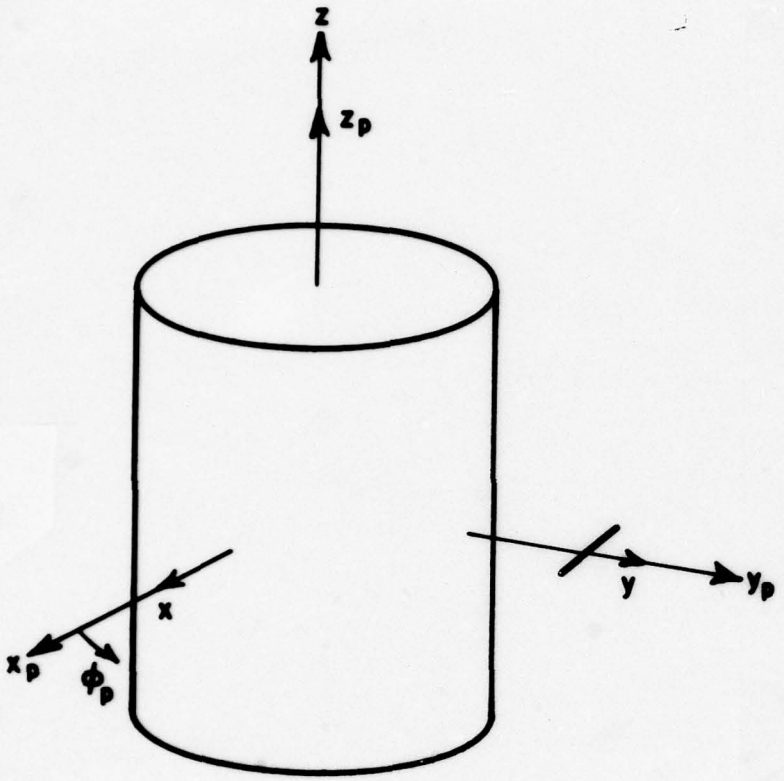

Figure 15a. An electric dipole in the presence of a finite circular cylinder (pattern taken in x-y plane).

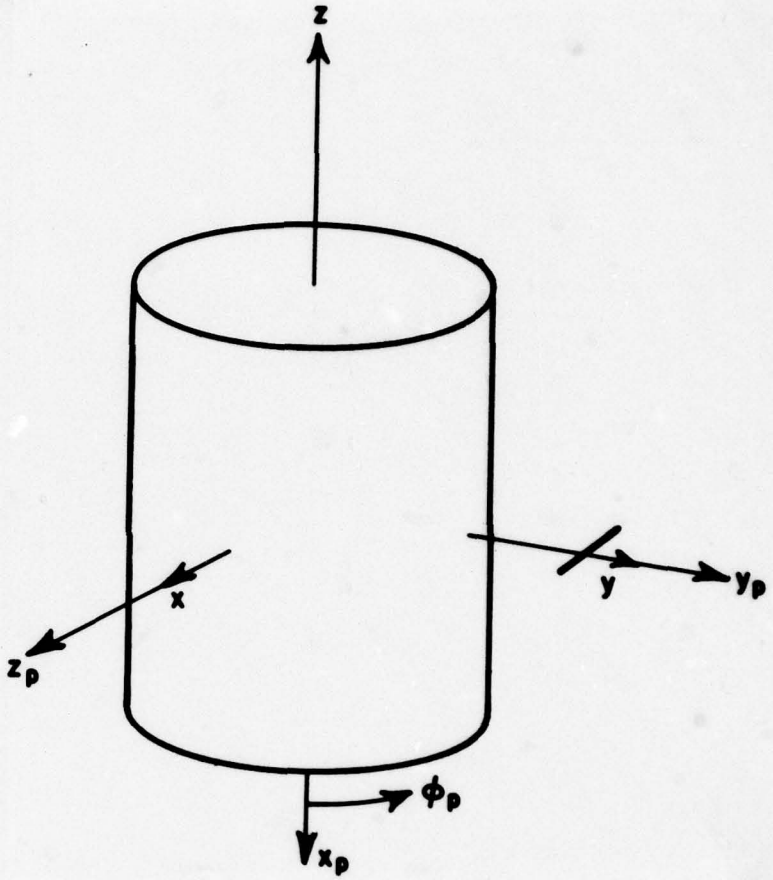

Figure 15b. An electric dipole in the presence of a finite circular cylinder (pattern taken in y-z plane).

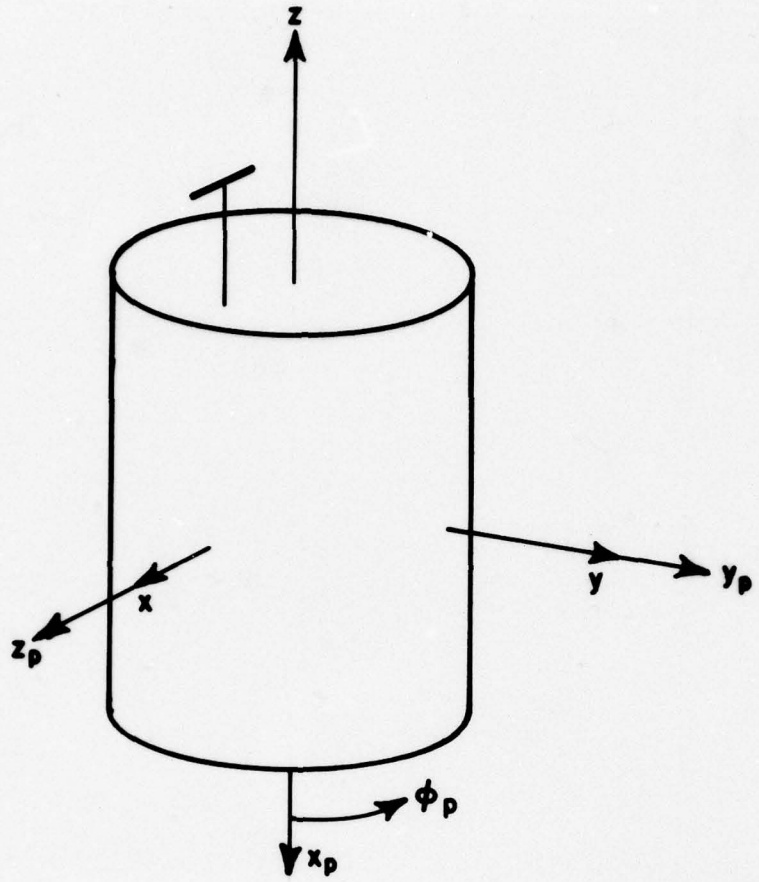

Figure 15c. An electric dipole in the presence of a finite circular cylinder (pattern in the y-z plane).

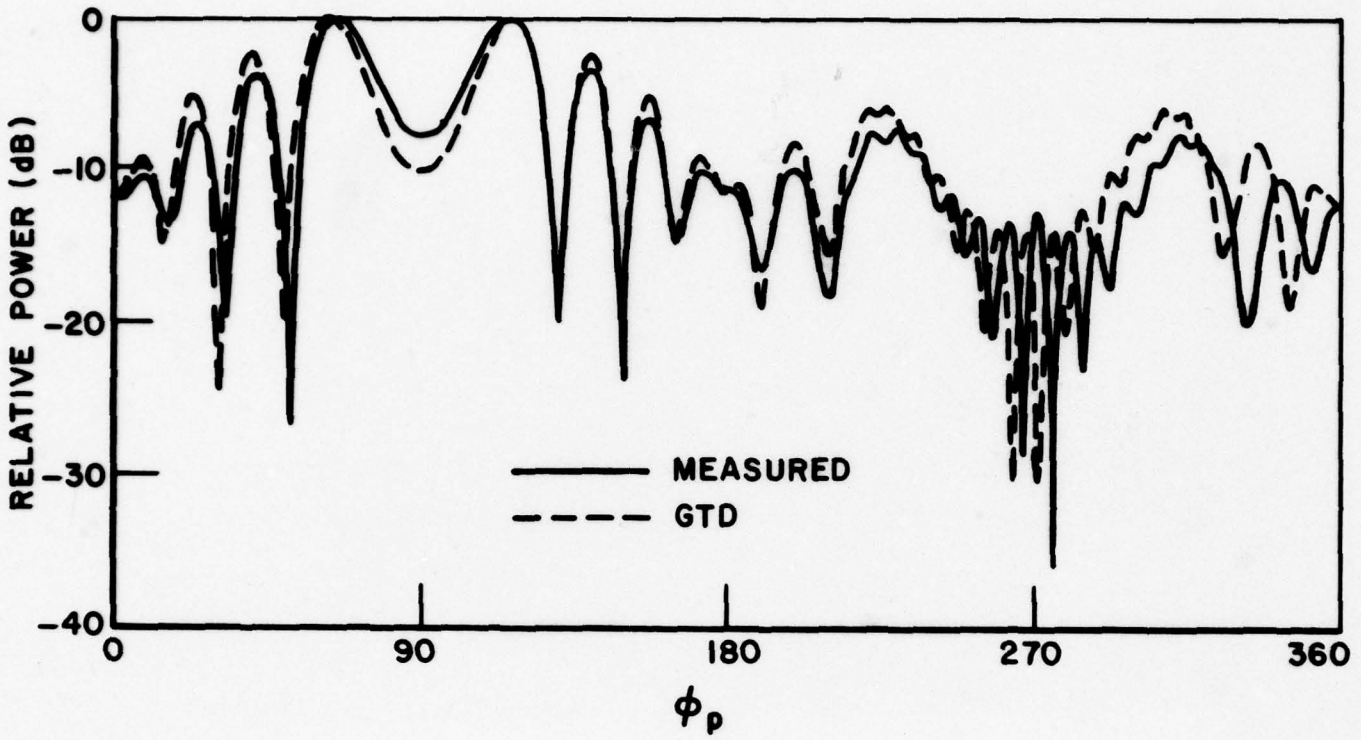

Figure 16a. Comparison of the measured (Bach) and calculated radiation pattern for $E_{\phi p}$ of an electric dipole on the y-axis parallel to the x-axis in the presence of a finite circular cylinder (pattern taken in x-y plane).

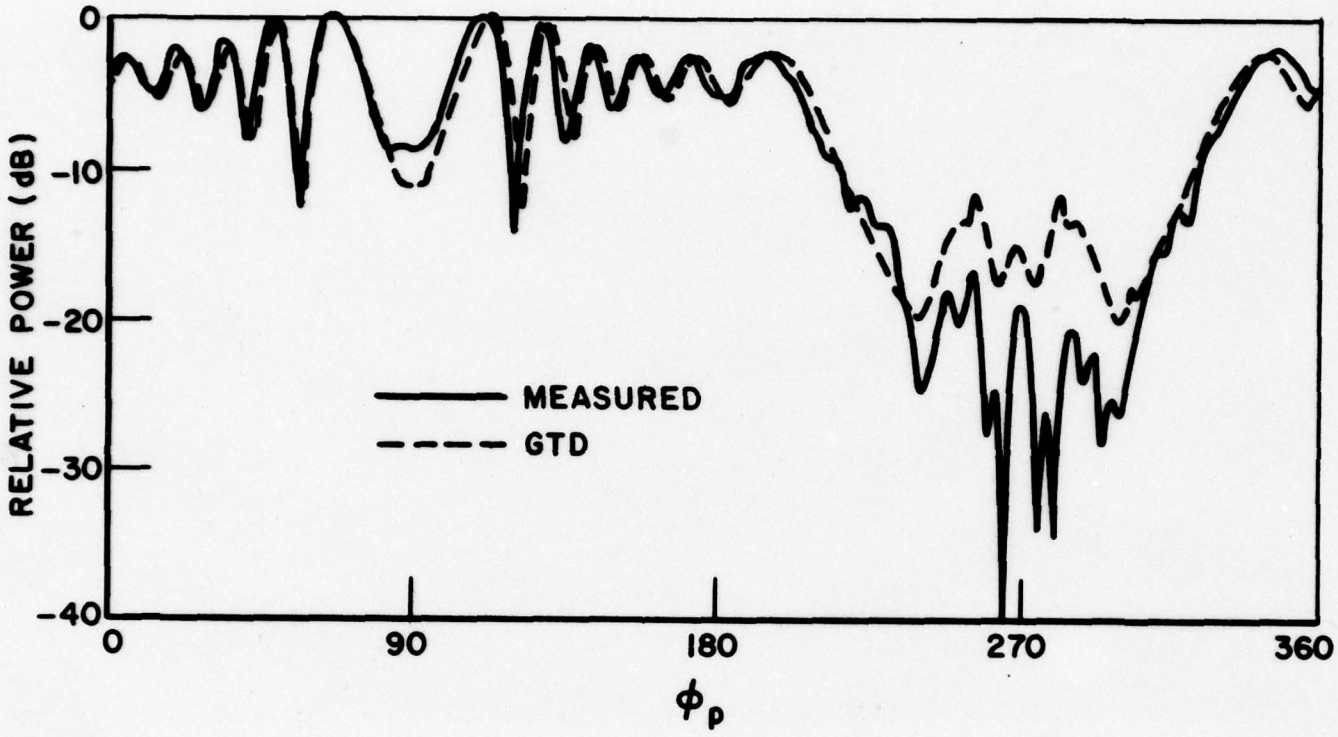

Figure 16b. Comparison of the measured (Bach) and calculated radiation pattern for $E_{\theta p}$ for an electric dipole on the y-axis parallel to the x-axis in the presence of a finite circular cylinder (pattern taken in y-z plane).

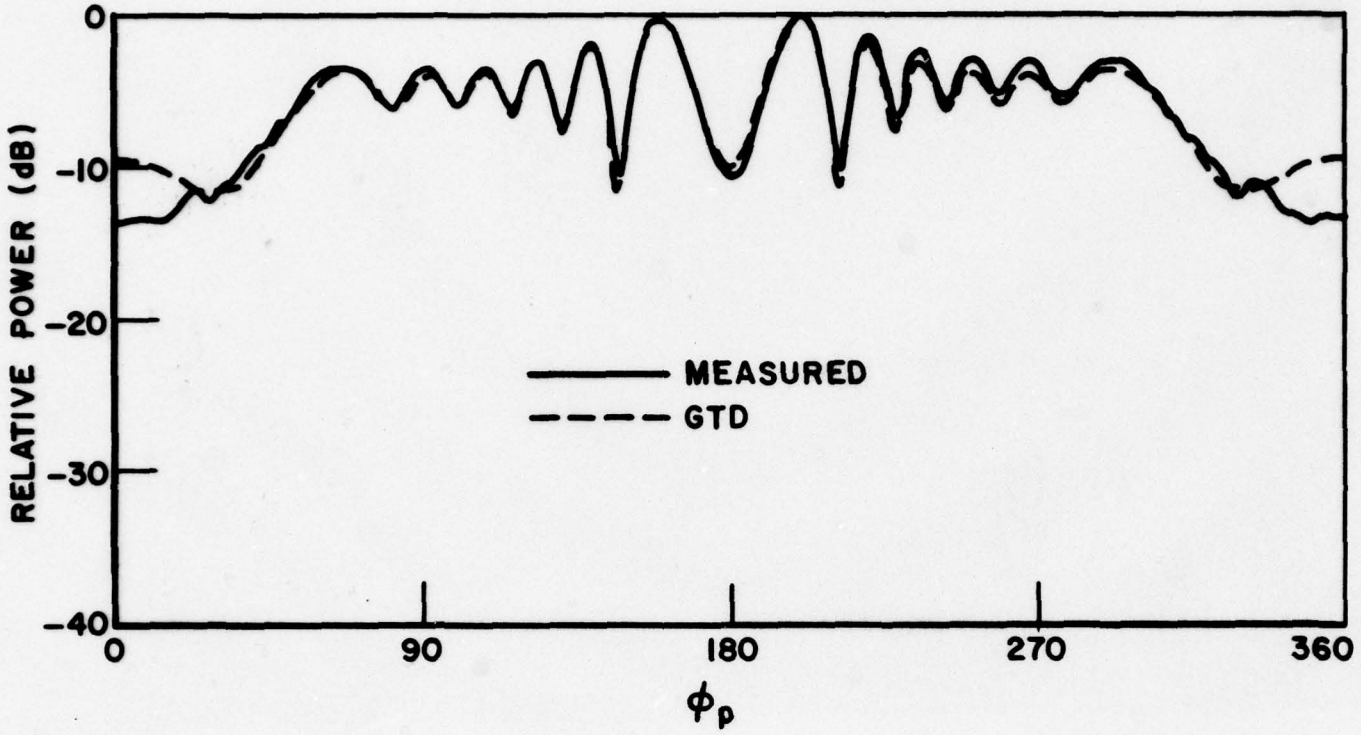

Figure 16c. Comparison of the measured (Bach) and calculated radiation pattern for $E_{\theta p}$ of an electric dipole in the x-z plane parallel to the x-axis in the presence of a finite circular cylinder (pattern taken in the y-z plane).

Example 5. Consider the pattern of a magnetic dipole in the presence of an elliptic cylinder as shown in Figure 17. The input data is given by:

```
PD:
0.,0.,90.
0,360,1
0.2997925
CG:
T
2.,1.,1
-500.,90.,500.,90.
SG:
1,1
2.828,2.828,0.
1,0.5,0.,0.
1.,0.
EX:
```

The $E_{\phi p}$ pattern is plotted in Figure 18 compared with a moment method solution. The $E_{\theta p}$ pattern is not plotted because it is of negligible value.

Example 6. This example illustrates the analysis of the pattern of an electric dipole in the presence of a plate and a finite circular cylinder as shown in Figure 19. The patterns of the individual parts are first analyzed separately and then combined to see the effects of the different structures. The following input is shown as if all four cases are run consecutively in one run. Of course, the input could easily be constructed for individual runs for each case.

```
TO:
F,F,F
F,F,T
1,7,1,3,1,4
PD:
0.,0.,90.
0,360,1
4.
SG:
1,3
0.,5.625,0.
0,0.508,90.,0.
1.,0.
EX:
```

6a. Source alone (Figure 20a)

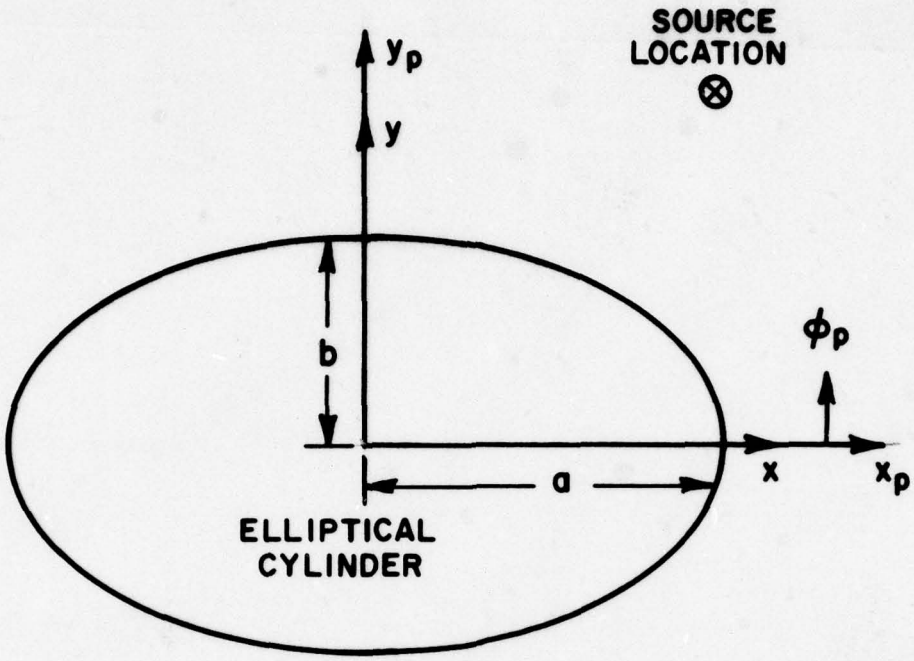

Figure 17. Elliptic cylinder configuration excited by a magnetic source parallel to the z-axis.

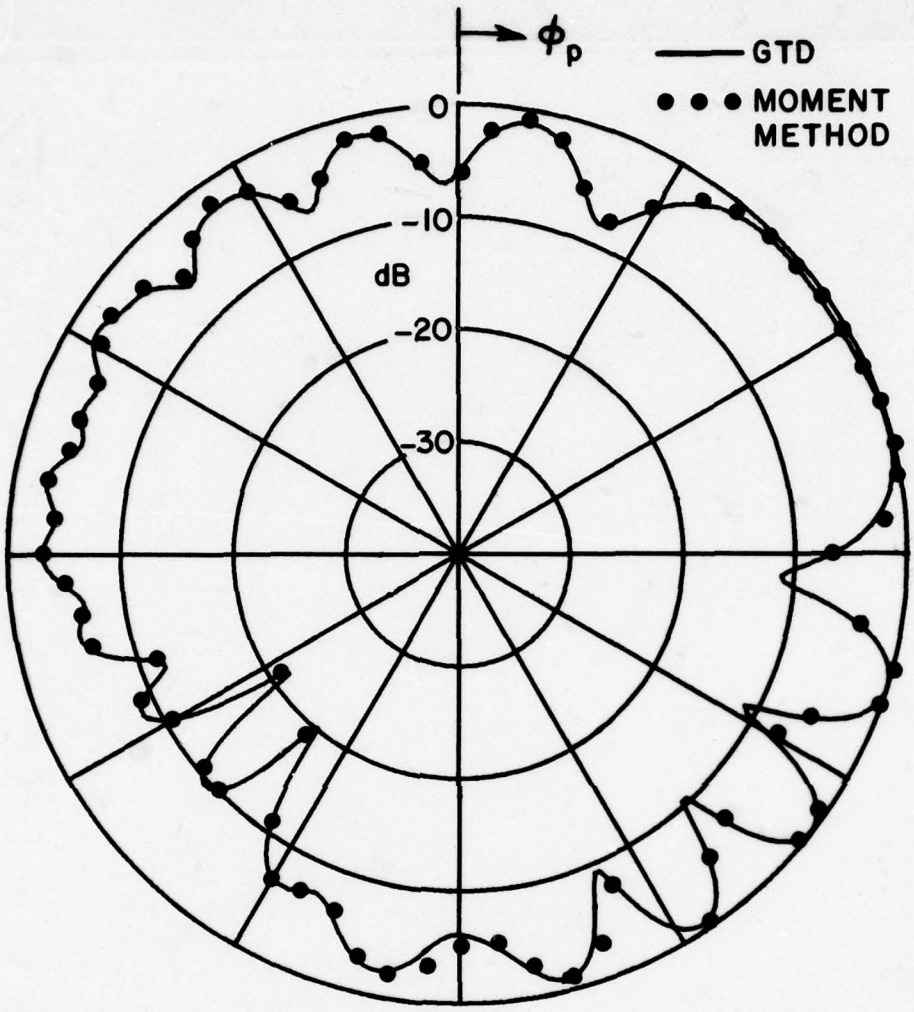

Figure 18. Comparison of GTD and moment method results ($E_{\phi p}$ pattern) for an elliptic cylinder (a=2, b=1).

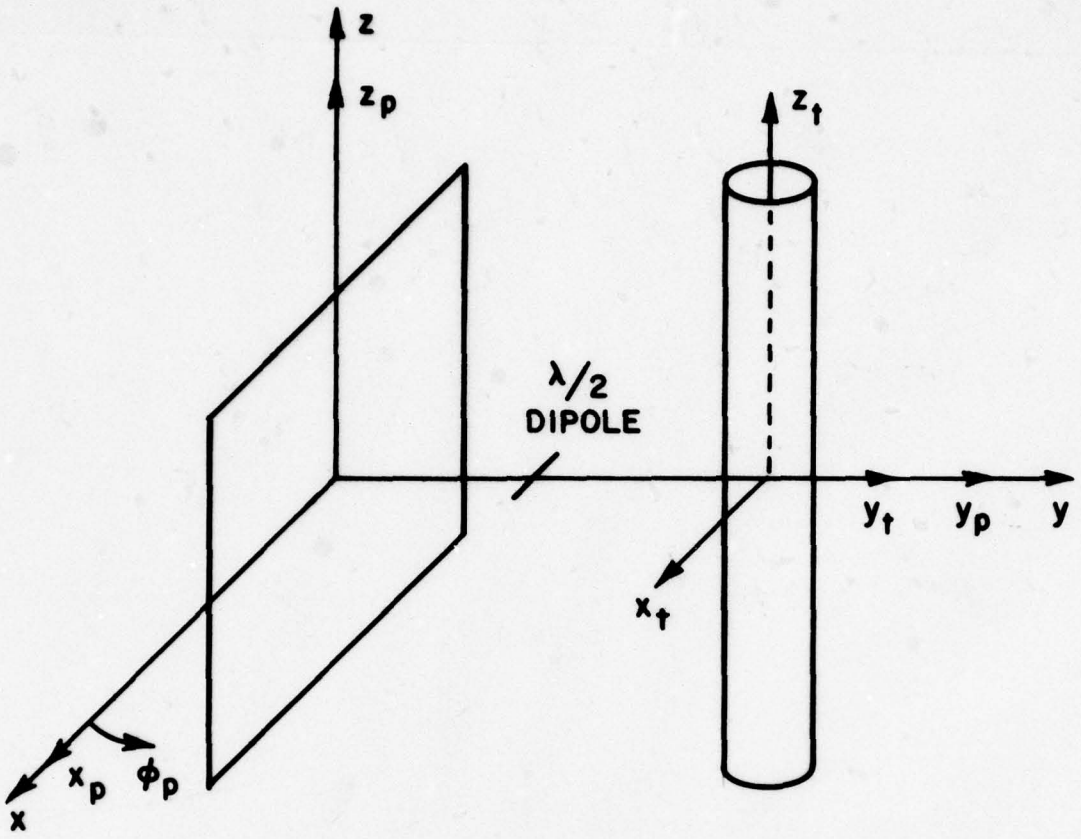

Figure 19. A λ/2 dipole in the presence of a square plate.

```
TO:
F,F,F
T,T,F
1,7,1,3,1,4
PG:
T
1,3
4
5.,0.,5.
5.,0.,-5.
-5.,0.,-5.
-5.,0.,5.
```

6b. Source and plate (Figure 20b)

```
EX:
PG:
F
RT:
3,0.,12.3125,-0.125
0.,0.,90.,0.
CG:
T
1.25,1.25,3
-8.5,90.,8.5,90.
```

6c. Source and cylinder (Figure 20c)

```
EX:
RT:
3,0.,0.,0.
0.,0.,90.,0.
PG:
T
1,3
4
5.,0.,5.
5.,0.,-5.
-5.,0.,-5.
-5.,0.,5.
EX:
```

6d. Source, plate, and cylinder (Figure 20d)

The $E_{\phi p}$ pattern is compared between the calculated and measured patterns for the source alone in Figure 20a, the source and plate in Figure 20b, the source and cylinder in Figure 20c, and the source, plate, and cylinder in Figure 20d.

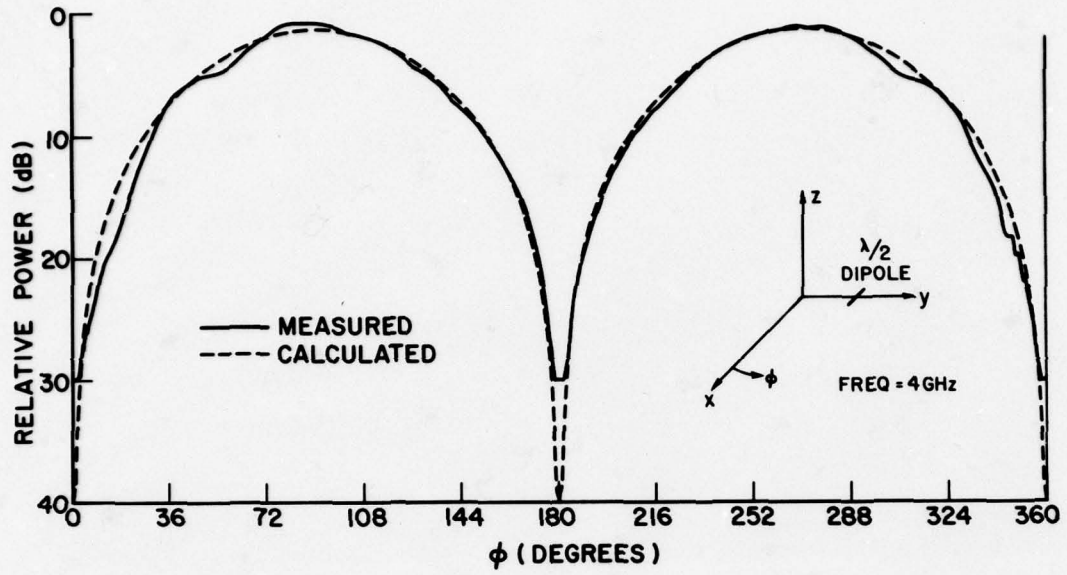

Figure 20a. Comparison of the measured and calculated E_ϕ radiation pattern of a $\lambda/2$ dipole.

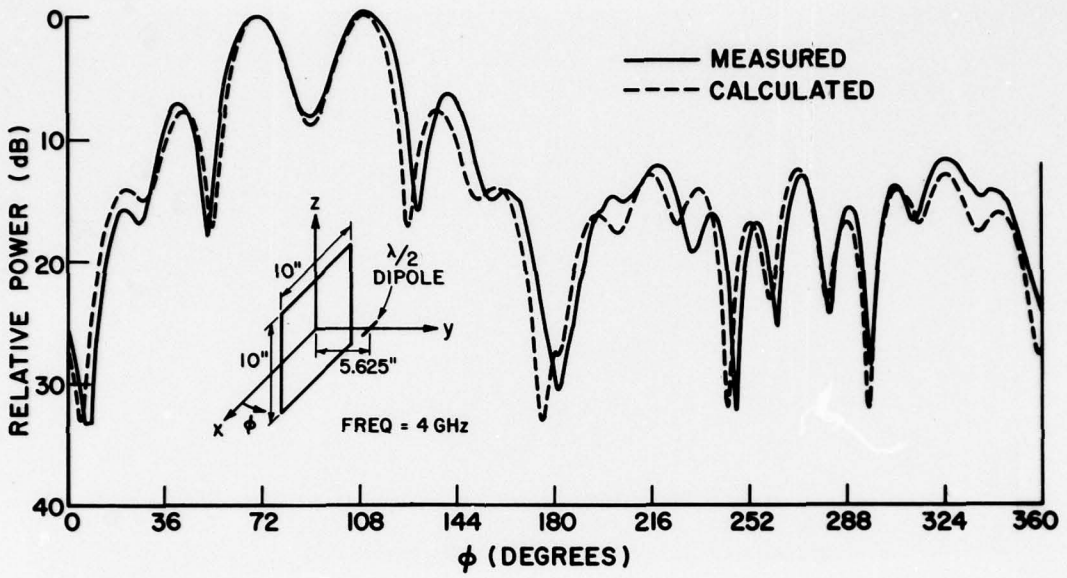

Figure 20b. Comparison of the measured and calculated E_ϕ radiation pattern of a dipole in the presence of a square plate.

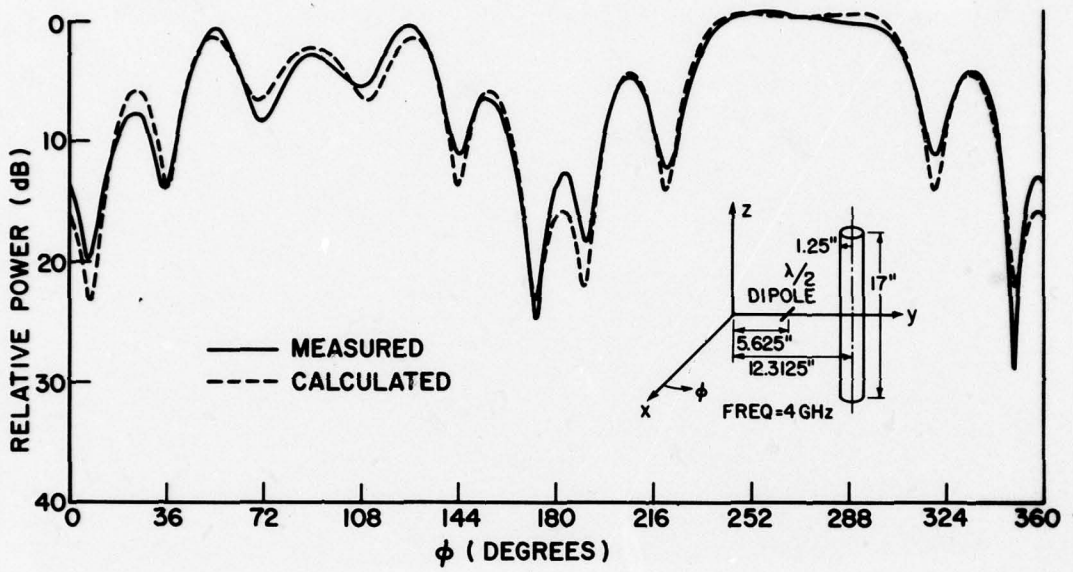

Figure 20c. Comparison of the measured and calculated E_ϕ radiation pattern of a dipole in the presence of a finite circular cylinder.

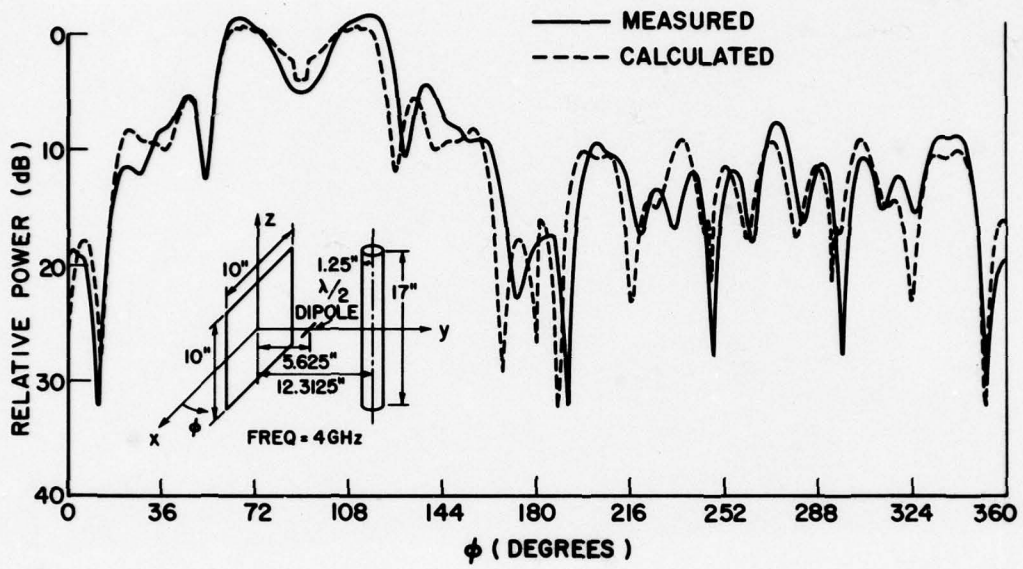

Figure 20d. Comparison of the measured and calculated (with plate-cylinder interactions) E_ϕ radiation pattern of a dipole in the presence of a square plate and a finite circular cylinder.

Example 7. Consider an electric monopole mounted on the wing of a simple aircraft model as shown in the insert of Figure 21. The input data is given by:

```
CM:     INPUT FOR A SIMPLE AIRCRAFT MODEL
CE:     COMPARISON OF MEASURED RESULTS
PD:
0.,0.,90.
0,360,1
10.87
PG:
T
2,3
4,4
0.,15.31,-15.81
0.,15.31,-12.81
0.,2.5,0.
0.,2.5,-6.
0.,-2.5,-6.
0.,-2.5,0.
0.,-15.31,-12.81
0.,-15.31,-15.81
SG:
1,3
0.,7.5,-7.19
0,0.5,90.,0.
1.,0.
CG:
T
2.5,2.5,3
-30.5,90.,17.5,90.
EX:
```

The $E_{\phi p}$ pattern is compared with a measured result in Figure 21. The $E_{\theta p}$ pattern is not plotted because it is of negligible value.

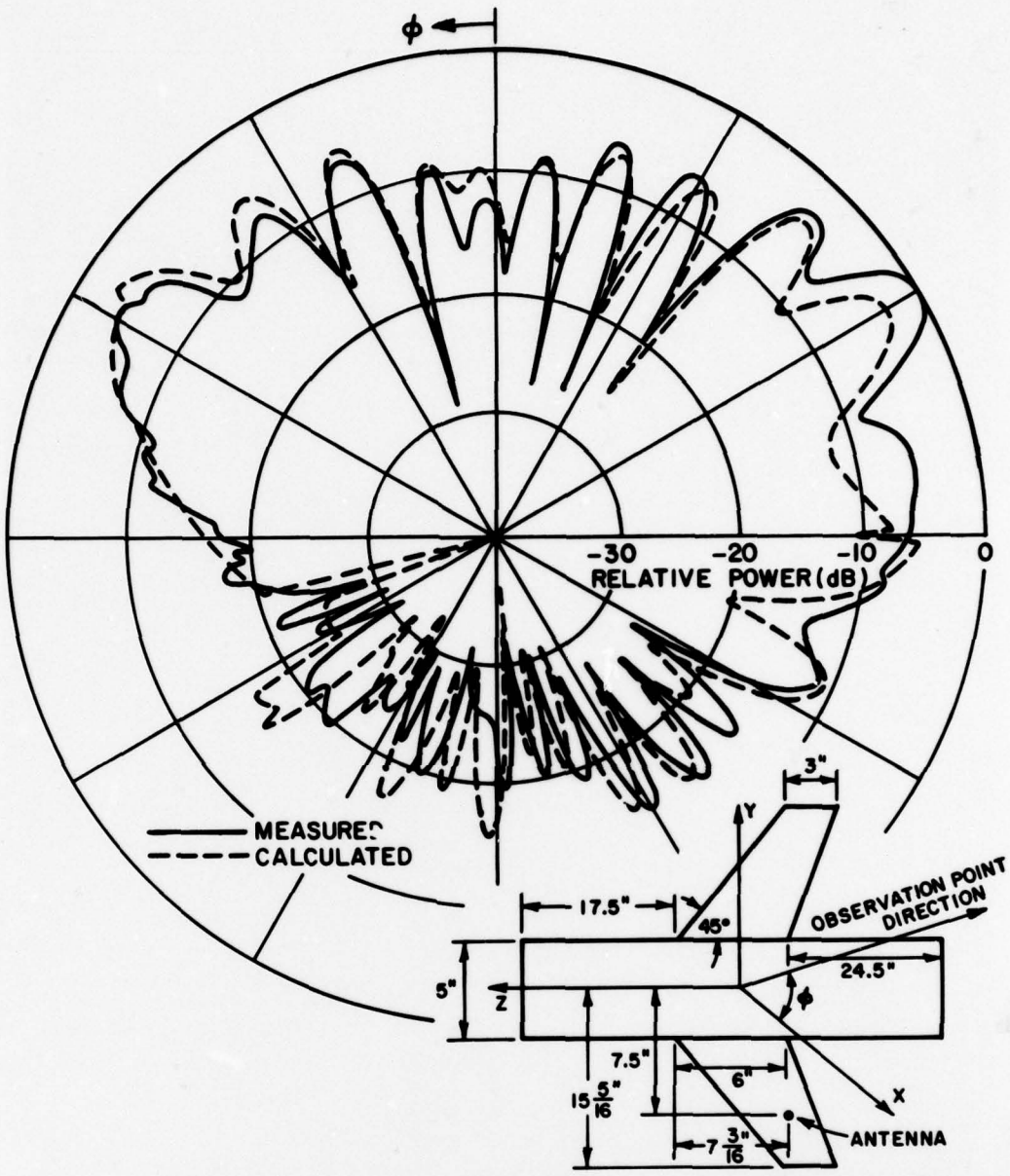

Figure 21. Comparison of measured and calculated results for the roll plane radiation pattern (E_ϕ) of a simple aircraft model with a short monopole mounted on its wing. (freq = 10.87 GHz).

Example 8. Consider a slot mounted on the wing of a F-4 aircraft. The computer model of the F-4 is illustrated in Figure 22. The input data is given by:

```
CM:     INPUT FOR A F4 COMPUTER MODEL
CE:     COMPARISON OF MEASURED RESULTS
CG:       FUSELAGE INPUT
T
87.,54.,3
-420.,90.,26.6,20.
PG:     WINGS AND VERTICAL STABILIZER INPUT
T
5,3
4,5,4,5,4
0.,54.,-228.
0.,166.2,-86.2
0.,166.2,32.8
0.,54.,0.
0.,166.2,-86.2
0.,166.2,-96.2
19.7,228.7,0.
19.7,228.7,53.4
0.,166.2,32.8
0.,-54.,0.
0.,-166.2,32.8
0.,-166.2,-86.2
0.,-54.,-228.
0.,-166.2,32.8
19.7,-228.7,53.4
19.7,-228.7,0.
0.,-166.2,-96.2
0.,-166.2,-86.2
87.,0.,205.1
149.9,0.,197.3
154.3,0.,153.1
87.,0.,11.4
SG:     .748 WAVELENGTH SLOT
1,3
0.,149.1,-73.6
1,0.748,135.,90.
1.,0.
PD:     MAIN BEAM ELEVATION
45.,270.,90.
0,360,1
.5
EX:
```

The $E_{\phi p}$ radiation pattern is compared with a measured result made on a scale model of a F-4 at Naval Weapons Center [5], in Figure 23.

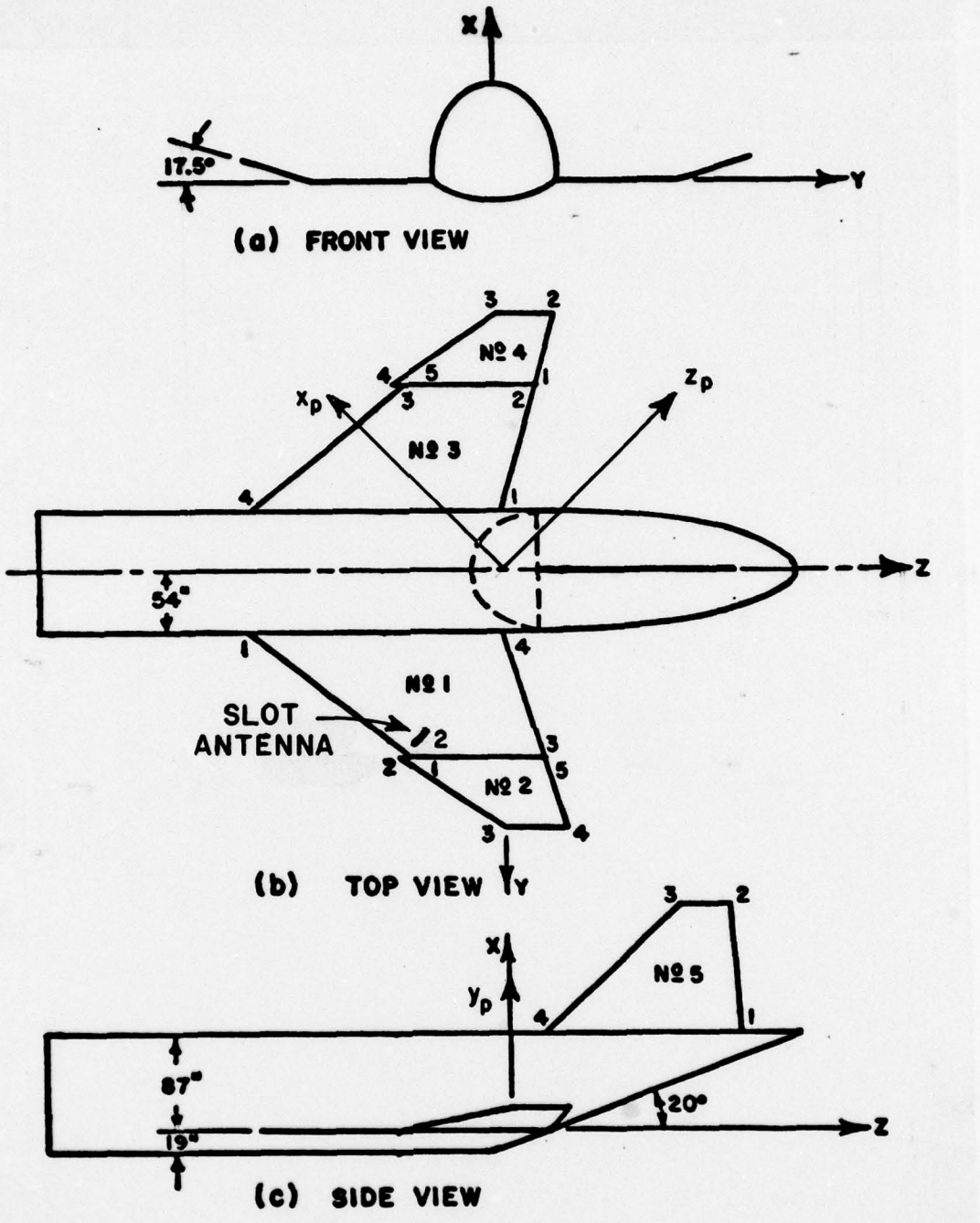

Figure 22. Illustration of geometry of F-4 aircraft model used in finite elliptic cylinder model.

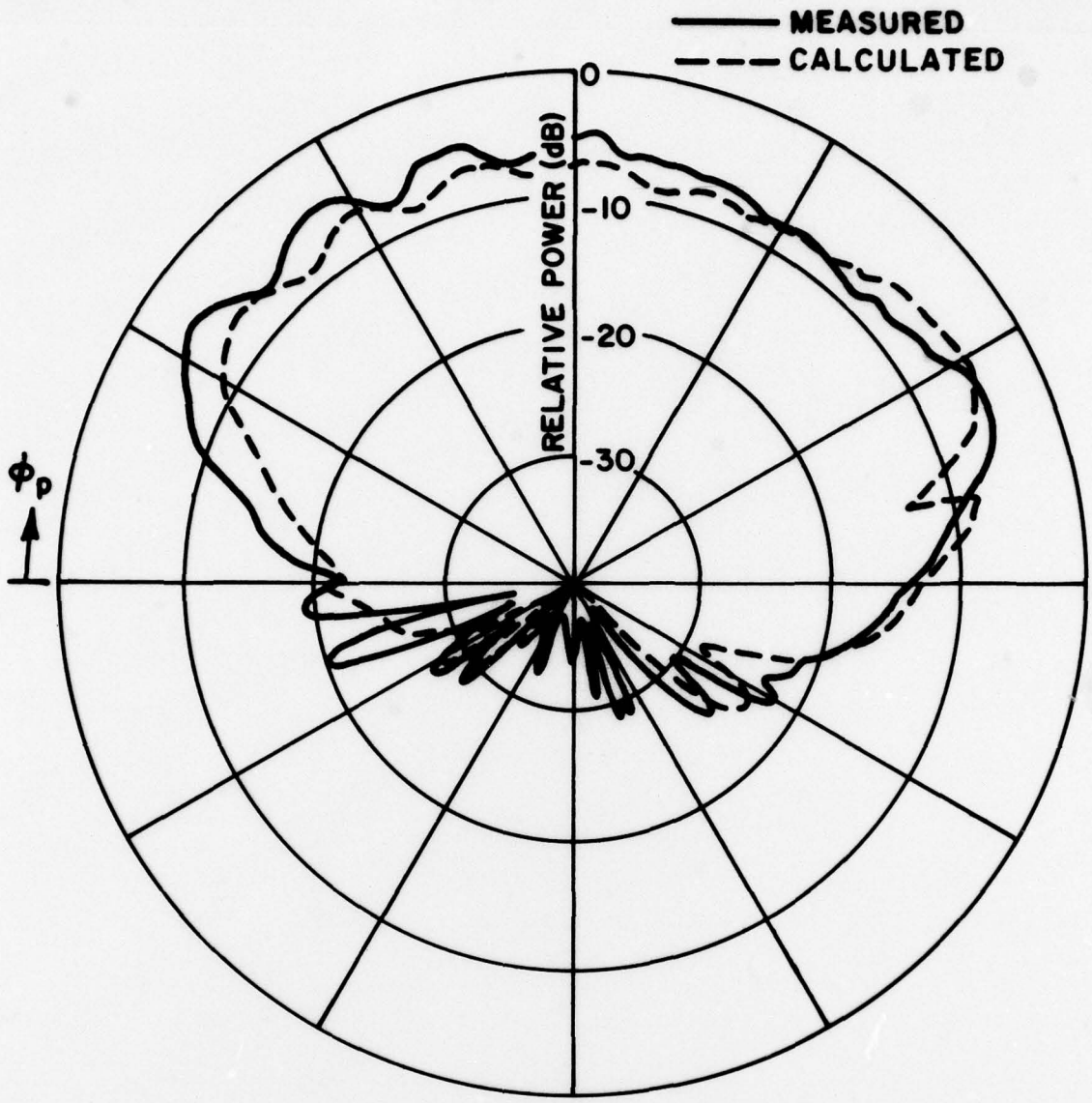

Figure 23. Comparison of NWC measured results on an F-4 model with the finite elliptic cylinder model results of main beam elevation plane radiation pattern.

Example 9. Consider a slot mounted on the wing of a Boeing 737 aircraft. The computer model of the Boeing 737 is illustrated in Figure 24. The input data is given by:

```
CM:     INPUT FOR A BOEING 737 COMPUTER MODEL
CE:     COMPARISON OF MEASURED RESULTS
PD:
60.,90.,90.
0,360,1
1.746
CG:
T
104.1,74.7,3
-570.5,90.,260.4,20.
PG:
T
3,3
5,5,4
0.,74.7,-212.8
0.,547.9,40.8
0.,547.9,95.1
0.,203.8,0.
0.,74.7,0.
0.,-74.7,0.
0.,-203.8,0.
0.,-547.9,95.1
0.,-547.9,40.8
0.,-74.7,-212.8
104.1,0.,448.3
344.1,0.,516.2
344.1,0.,443.7
104.1,0.,235.5
SG:
3,3
0.,312.4,-45.3
1,0.827837,90.,90.
1.,0.
0.,312.4,-44.366
1,0.827837,90.,90.
1.,0.
0.,312.4,-46.234
1,0.827837,90.,90.
1.,0.
EX:
```

The $E_{\phi p}$ radiation pattern is compared with measurements in Figure 25. The measurements were made on a 1/20 scale model of a Boeing 737 at NASA (Hampton, Virginia). The antenna is a KA band waveguide mounted in the wing and is represented by three magnetic dipoles in the computer results [5].

The line printer output for this example is shown in Figure 26. This is only a partial list of the output for the fields above the wing in 10° increments for brevity.

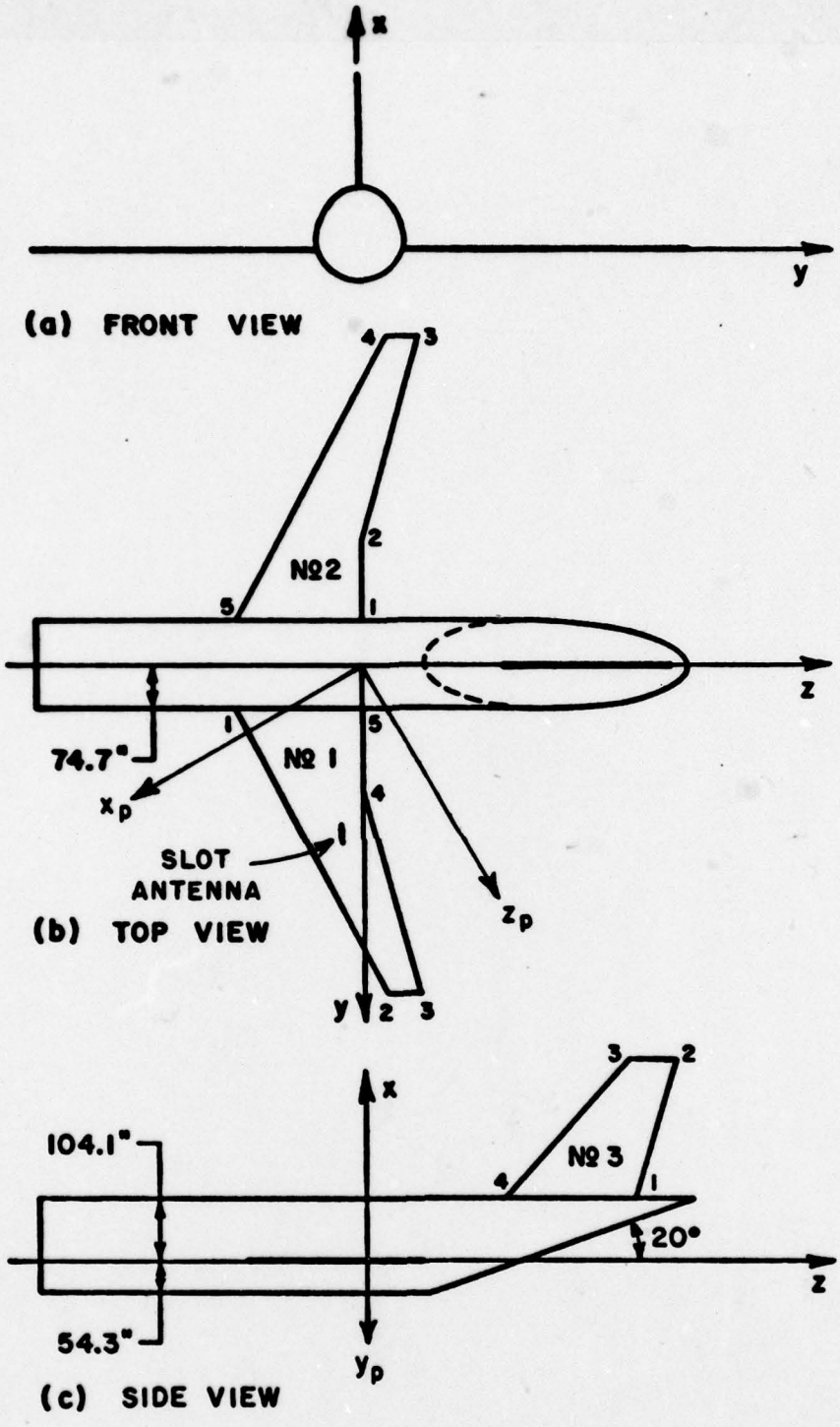

Figure 24. Illustration of geometry of Boeing 737 aircraft model used in finite elliptic cylinder model.

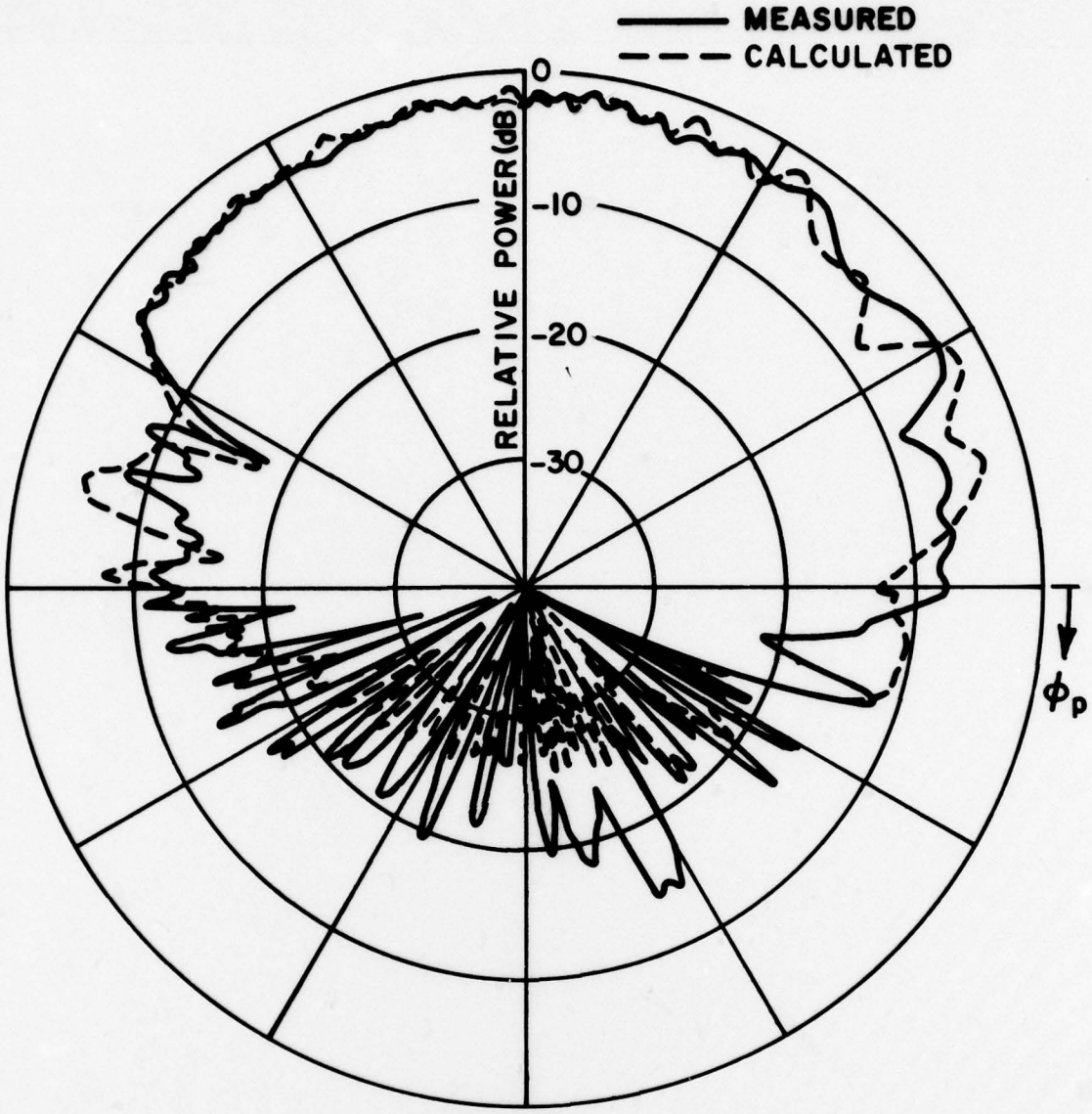

Figure 25. Comparison of measured and calculated E_{θ_p} results.

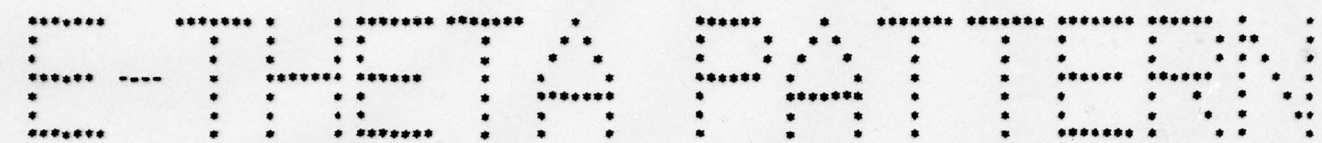

ROTATED COORDINATES (THO = 60.00000 , PHO = 90.00000)

CAUTION THE DIRECTIVE GAIN IS BASED ON A CRUDE ESTIMATE OF THE POWER RADIATED FROM ISOLATED DIPOLES

THETA	PHI	E-THETA	PHASE	UNNORMALIZED MAGNITUDE	UNNORMALIZED DB GAIN	NORMALIZED MAGNITUDE	NORMALIZED DB
90.00000	180.00000	-.17801E -1 -.29878E -1	-120.78610	.34778E -1	-32.13342	.04156	-27.62655
90.00000	190.00000	-.48441E -1 .19234E -1	158.34420	.52120E -1	-28.61957	.06228	-24.11270
90.00000	200.00000	-.11834E 0 -.43871E -1	-159.65898	.12621E 0	-20.93782	.15082	-16.43096
90.00000	210.00000	-.15511E 0 -.2_943E 0	-124.90606	.26757E 0	-11.41096	.31974	-9.90410
90.00000	220.00000	-.34003E 0 -.13514E 0	-158.32574	.36590E 0	-11.69247	.43724	-7.18560
90.00000	230.00000	.15694E 0 .56283E 0	74.41979	.58430E 0	-7.62687	.69823	-3.12080
90.00000	240.00000	-.59263E -1 .58768E 0	95.75838	.59066E 0	-7.53288	.70583	-3.02601
90.00000	250.00000	.54980E 0 -.45885E 0	-39.84779	.71611E 0	-5.85997	.85575	-1.35311
90.00000	260.00000	-.58269E -1 -.83555E 0	-92.62245	.83683E 0	-4.50667	1.00000	-.00000
90.00000	270.00000	-.27690E -1 -.72473E 0	-92.18810	.72526E 0	-5.74978	.86667	-1.24291
90.00000	280.00000	.81248E -1 -.80569E 0	-84.24164	.80978E 0	-4.79225	.96768	-.28538
90.00000	290.00000	-.48132E 0 -.53655E 0	-131.69456	.72080E 0	-5.80326	.86135	-1.29641
90.00000	300.00000	.19267E 0 .63406E 0	73.09778	.66269E 0	-6.53543	.79190	-2.02858
90.00000	310.00000	-.58002E 0 .47871E 0	128.44436	.61121E 0	-7.28581	.73039	-2.72894
90.00000	320.00000	.37165E 0 -.36983E 0	-46.36712	.53860E 0	-8.53423	.64362	-3.82736
90.0000	330.00000	.20043E 0 -.22510E 0	-48.31862	.30140E 0	-10.37664	.36017	-8.86977
90.00000	340.00000	.24985E 0 -.16882E 0	-34.04547	.30154E 0	-10.37270	.36034	-8.86583
90.00000	350.00000	.41959E -1 .49389E -1	43.19037	.57551E -1	-27.75059	.06877	-23.25172
90.00000	360.00000	-.55986E -1 -.12908E -1	-167.01654	.57455E -1	-27.77302	.06866	-23.26615

Figure 26a. Partial listing of the line printer output for the $E_{\theta p}$ fields of a slot mounted on the wing of a Boeing 737.

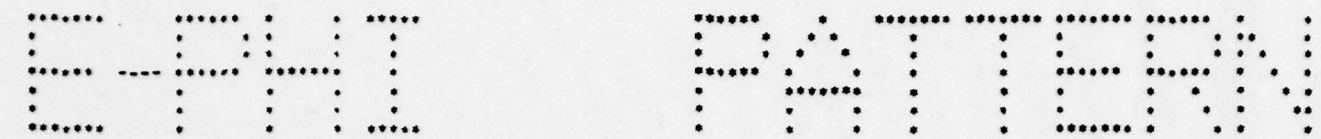

ROTATED COORDINATES (THO = 90.00000 , PHO = 90.00000)

CAUTION THE DIRECTIVE GAIN IS BASED ON A CRUDE ESTIMATE OF THE POWER RADIATED FROM ISOLATED DIPOLES

THETA	PHI	E-PHI		PHASE	UNNORMALIZED MAGNITUDE		DB GAIN	NORMALIZED MAGNITUDE	DB
90.00000	180.00000	.1516BE	0	-88.16204	.65401E	0	-11.97946	.25687	-12.30979
90.00000	190.00000	-.14207E	0	101.38367	.61844E	0	-7.16467	.41581	-7.66400
90.00000	200.00000	-.57665E	0	-173.08252	.60289E	0	-7.35488	.40340	-7.88521
90.00000	210.00000	-.25049E	1	-110.25836	.72644E	0	-5.77156	.46407	-6.50191
90.00000	220.00000	-.96660E	0	-148.45827	.11752E	1	-1.55766	.78653	-2.08795
90.00000	230.00000	.40861E	0	57.56303	.11347E	1	-1.88216	.75923	-2.39249
90.00000	240.00000	-.15225E	0	.12267E	1	104.38824	.12685E	1	-.89553	.84886	-1.42366
90.00000	250.00000	-.10436E	0	-.90597E	0	-45.05085	.12801E	1	-.81477	.85653	-1.34510
90.00000	260.00000	-.14956E	-1	-.13502E	1	-93.76934	.13542E	1	-.48265	.90542	-.86297
90.00000	270.00000	.13644E	-1	-.12919E	1	-89.19978	.12920E	1	-.73427	.86451	-1.26460
90.00000	280.00000	-.19347E	0	-.12547E	1	-82.22865	.13672E	1	-.24264	.91483	-.77317
90.00000	290.00000	-.03592E	0	-.11652E	1	-128.77319	.14945E	1	.53063	1.00000	-.00000
90.00000	300.00000	.21494E	0	.10313E	1	72.91829	.10789E	1	-2.25559	.72184	-2.82992
90.00000	310.00000	-.46498E	0	.86904E	0	118.14911	.98562E	0	-3.08544	.65950	-3.61576
90.00000	320.00000	-.73535E	0	-.57669E	0	-24.38528	.91722E	0	-3.71816	.61373	-4.24149
90.00000	330.00000	-.35782E	-1	-.12533E	1	-94.57022	.12570E	1	-.97510	.84106	-1.50545
90.00000	340.00000	.16044E	0	-.38303E	0	-23.98410	.94229E	0	-3.47587	.63051	-4.00621
90.00000	350.00000	-.78594E	-1	.89549E	0	95.01978	.89898E	0	-3.88505	.60149	-4.41537
90.00000	360.00000	-.18069E	0	-.36524E	0	-116.32461	.40750E	0	-10.75712	.27266	-11.28745

Figure 26b. Partial listing of the line printer output for the $E_{\phi p}$ fields of a slot mounted on the wing of a Boeing 737.

TOTAL DIRECTIVE GAIN IN DB

CAUTION THE DIRECTIVE GAIN IS BASED ON A CRUDE ESTIMATE OF THE POWER RADIATED FROM ISOLATED DIPOLES

ROTATED COORDINATES (THO = 60.00000 , PHO = 90.00000)

THETA	PHI	MAJOR	MINOR	TILT ANG	AXIAL RATIO	TOTAL GAIN	NORM GAIN
90.00000	180.00000	-11.96395	-34.14520	86.56825	.07779	-11.93775	-13.37635
90.00000	190.00000	-7.12446	-30.16084	87.35603	.07050	-7.10293	-8.54154
90.00000	200.00000	-7.36922	-45.72154	78.19471	.01161	-7.36861	-8.80722
90.00000	210.00000	-5.24447	-26.87996	70.16929	.08284	-5.21477	-6.65537
90.00000	220.00000	-1.17357	-25.04698	74.05100	.06405	-1.15578	-2.59439
90.00000	230.00000	-.90247	-19.33921	64.35277	.11972	-.84066	-2.27927
90.00000	240.00000	-.05572	-24.84594	65.19316	.05761	-.04133	-1.47994
90.00000	250.00000	.36122	-27.88114	60.82917	.03670	.36772	-1.07088
90.00000	260.00000	1.07351	-39.86559	58.26856	.00695	1.07366	-.36475
90.00000	270.00000	.45416	-32.59507	60.71017	.02226	.45532	-.98329
90.00000	280.00000	1.06204	-35.18554	59.36791	.01541	1.06387	-.37554
90.00000	290.00000	1.43665	-31.98943	64.27456	.02152	1.43861	-.00000
90.00000	300.00000	-.90051	-57.90668	58.44189	.00141	-.90350	-2.34811
90.00000	310.00000	-1.70042	-25.57733	58.38185	.08057	-1.67232	-3.11093
90.00000	320.00000	-2.54448	-18.03522	60.51969	.16006	-2.42352	-3.86212
90.00000	330.00000	-.85098	-16.35253	80.27913	.16765	-.73031	-2.16892
90.00000	340.00000	-3.06368	-28.92089	72.46434	.05084	-3.05247	-4.49107
90.00000	350.00000	-3.57643	-29.85950	87.72642	.05025	-3.56720	-5.00579
90.00000	360.00000	-10.72220	-30.03566	84.83949	.10822	-10.67163	-12.11024

Figure 26c. Partial listing of the line printer output for the total directive gain of a slot mounted on the wing of a Boeing 737.

APPENDIX I

The following is a listing of a polar plot subroutine which can be used to generate the polar patterns given in Section IV. Note that this code refers to two subroutines "PLOTS" and "PLOT" which must be added by the system or operator. The definitions of these routines are given in the comments associated with the code.

```
      SUBROUTINE POLPLT(ET,RP,IPLT,IPHS,IDM)
C!!!
C!!!  THIS ROUTINE IS USED TO PLOT THE RESULTS IN TERMS OF A
C!!!  POLAR PLOT. THE CALL TO SUBROUTINE "PLOTS" IS USED TO INITIALIZE
C!!!  THE PLOTTER. THE CALLS TO THE SUBROUTINE "PLOT" ARE USED TO
C!!!  DRAW THE DATA AS FOLLOWS:
C!!!
C!!!        CALL PLOT(X,Y,N)
C!!!
C!!!        X,Y=COORDINATES OF THE NEW PLOT POINT.
C!!!
C!!!        N=2     PEN IS DOWN MOVING TO THE NEW POINT.
C!!!        N=3     PEN IS UP MOVING TO THE NEW POINT.
C!!!        N=999   BUFFER USED TO STORE PLOT DATA IS EMPTIED TO PLOTTER
C!!!
C!!!        N<0     IMPLIES ORIGIN SHIFT TO THE NEW POINT.
C!!!        N>0     IMPLIES NO ORIGIN SHIFT AFTER MOVING TO NEW POINT.
C!!!
      COMPLEX ET(IDM)
      DIMENSION IBUF(100)
      DATA PI,TPI,DPR/3.14159265,6.2831853,57.29577958/
      EMX=0.
      DO 101 IP=0,360,IPHS
      I=IP+1
      EM=CABS(ET(I))
      IF(EM.GT.EMX) EMX=EM
  101 CONTINUE
      CALL PLOTS(IBUF,100,3)
      CALL PLOT(4.25,5.5,-3)
C *** POLAR GRID ***
      DO 110 I=1,4
      RG=RP*I/4.
      CALL PLOT(RG,0.,3)
      DO 110 J=0,360,2
      ANG=J/DPR
      XX=RG*COS(ANG)
      YY=RG*SIN(ANG)
  110 CALL PLOT(XX,YY,2)
      DO 112 I=1,6
```

```
      ANG=(I-1)*PI/6.
      ANGS=ANG+PI
      ANGF=ANG
      IF(I.EQ.2*(I/2)) GO TO 111
      ANGS=ANG
      ANGF=ANG+PI
  111 CONTINUE
      XX=RP*COS(ANGS)
      YY=RP*SIN(ANGS)
      CALL PLOT(XX,YY,3)
      XX=RP*COS(ANGF)
      YY=RP*SIN(ANGF)
  112 CALL PLOT(XX,YY,2)
C *** PATTERN PLOT ***
      DO 120 IP=0,360,IPHS
      I=IP+1
      ETM=CABS(ET(I))/EMX
      IF(IPLT-2) 121,122,123
  121 RD=RP*ETM
      GO TO 125
  122 RD=RP*ETM*ETM
      GO TO 125
  123 IF(ETM.LT.0.01) ETM=0.01
      RD=20.*ALOG10(ETM)
      IF(RD.LT.-40.) RD=-40.
      RD=RP*(RD+40.)/40.
  125 CONTINUE
      ANG=IP/DPR
      XX=RD*SIN(ANG)
      YY=RD*COS(ANG)
      IPEN=2
      IF(I.EQ.1) IPEN=3
  120 CALL PLOT(XX,YY,IPEN)
      CALL PLOT(4.25,-5.5,-3)
  130 CONTINUE
      CALL PLOT(0.,0.,999)
      RETURN
      END
```

REFERENCES

[1] R. G. Kouyoumjian and P. H. Pathak, "A Uniform Geometrical Theory of Diffraction for an Edge in a Perfectly-Conducting Surface," Proc. IEEE, Vol. 62, November 1974, pp. 1448-1461.

[2] R. G. Kouyoumjian, "The Geometrical Theory of Diffraction and Its Applications," Numerical and Asymptotic Techniques in Electromagnetics, edited by R. Mittra, Spring-Verlag, New York, 1975.

[3] P. H. Pathak and W. D. Burnside, "A Uniform Asymptotic Result for the Scattering of Plane Waves by a Circular Cylinder," Report 3873-1, March 1976, The Ohio State University ElectroScience Laboratory, Department of Electrical Engineering; prepared under Contract N62269-74-C-0788 for Naval Air Development Center, Warminster, Pa.

[4] W. D. Burnside, M. C. Gilreath, R. J. Marhefka, and C. L. Yu, "A Study of KC-135 Aircraft Antenna Patterns," IEEE Trans. on Antennas and Propagation, Vol. AP-23, No. 3, May 1975, pp. 309-16.

[5] R. J. Marhefka, "Analysis of Aircraft Wing-Mounted Antenna Patterns," Report 2909-25, June 1976, The Ohio State University ElectroScience Laboratory, Department of Electrical Engineering; prepared under Grant No. NGL 36-008-138 for National Aeronautics and Space Administration.

[6] W. D. Burnside, R. G. Kouyoumjian, R. J. Marhefka, R. C. Rudduck, and C. H. Walter, "Asymptotic High Frequency Techniques for UHF and Above Antennas," Annual Report 4508-6, August 1977, The Ohio State University ElectroScience Laboratory, Department of Electrical Engineering; prepared under Contract N00123-76-C-1371 for Naval Regional Procurement Office.

[7] W. D. Burnside, "User's Manual Flat Plate Program," Report 4508-4, May 1977, The Ohio State University ElectroScience Laboratory, Department of Electrical Engineering; prepared under Contract N00123-76-C-1371 for Naval Regional Procurement Office, Long Beach, California.

[8] R. J. Marhefka, "User's Manual for Plates and Cylinder Computer Code," Report 4508-8, March 1978, The Ohio State University ElectroScience Laboratory, Department of Electrical Engineering; prepared under Contract N00123-76-C-1371 for Naval Regional Procurement Office, Long Beach, California.

[9] C. H. Walter, Traveling Wave Antennas, Dover Publications, Inc., New York, 1970, pp. 15-16.

[10] J. D. Kraus, Antennas, McGraw Hill Co., Inc., New York, 1950, pp. 464-477.

[11] MBA Associates, "Antenna Modeling Program Systems Manual," Report MB-R-74162 San Ramon, California, 94583.

[12] H. Bach, "Pattern Measurements of High Frequency Satellite-Mounted Antennas," Electromagnetic Institute, Technical University of Denmark, R154, January 1976.